Mem. Descr. Carta Geol. d'It.
104 (2019), pp. 41 - 74
figg. 13, tabb. 4

Seafloor hydrothermal systems and associated mineral deposits of the Tyrrhenian Sea

Sistemi idrotermali sottomarini e depositi minerali associati del Mar Tirreno

MONECKE T.([1]), PETERSEN S.([2]),
AUGUSTIN N.([2]), HANNINGTON M.([2])

ABSTRACT - The Aeolian island arc in the southeastern Tyrrhenian Sea represents a ~180 km long chain of seven volcanic islands and several submerged volcanoes extending along the continental shelf of northern Sicily and western Calabria. Seafloor hydrothermal activity forming sulfate and sulfide deposits has been discovered on three of the arc volcanoes. This includes a subseafloor replacement-style barite and sulfide occurrence at ~630-650 m water depth at the Palinuro seamount in the eastern sector of the island arc. Drilling has shown that the subseafloor deposit is zoned with depth. The top of the mineralized zone is composed of barite and polymetallic sulfides, whereas the lower portion of the mineralized zone is dominated by massive pyrite that has distinctly lower base and precious metal grades. The deposit formed from hydrothermal fluids having an intermediate-sulfidation state, although excursions to high- and very high-sulfidation states are indicated by the presence of abundant enargite and hypogene covellite. The sulfidation state of the sulfide minerals and their sulfur isotopic compositions are indicative of a magmatic volatile contribution to the ore-forming hydrothermal fluids. Low-temperature Fe-rich deposits as well as sulfate and polymetallic sulfide deposits also occur in shallow water off Panarea in the eastern sector of the Aeolian island arc. Drilling showed that subcropping hydrothermal deposits in an area pockmarked by hydrothermal gas eruption craters at a water depth of ~55-85 m consist primarily of anhydrite and gypsum with minor barite, marcasite, pyrite, sphalerite, as well as alunite and kaolinite. Hydrothermal discharge at 23.5 m below sea-level resulted in the formation of hydrothermal precipitates consisting of galena, sphalerite, and barite. Hydrothermal venting also occurs in the littoral zone of Vulcano where marcasite and pyrite form through infiltration and replacement of the beach sands. Venting of thermal waters in the shallow waters at Panarea and Vulcano is accompanied by the widespread release of CO_2 causing an acidification of the seawater. The high gas flux and fluid chemistry suggest the existence of an actively degassing magma below the two islands. In addition to the three hydrothermal systems in the volcanic arc, low-temperature hydrothermal activity and the discharge of thermal waters has been discovered on the summit of the Marsili seamount at ~500 m water depth. Recovery of massive pyrite by dredging suggests the existence of a hitherto undiscovered high-temperature vent site at the spreading center. The vent sites of the Aeolian archipelago provide natural laboratories for the study of magmatic-hydrothermal processes occurring at variable water depths. The observation that sulfate and sulfide deposits on the Aeolian arc volcanoes primarily form by subseafloor replacement processes or are buried below sedimentary deposits whereas hydrothermal precipitates on the back-arc form at the seafloor on top of massive lavas highlights volcanic facies controls on the nature of min-

([1]) Center for Mineral Resources Science, Department of Geology and Geological Engineering, Colorado School of Mines, 1516 Illinois Street, Golden, Colorado, 80401, U.S.A.
([2]) GEOMAR, Helmholtz Centre for Ocean Research Kiel, Wischofstrasse 1-3, D-24148 Kiel, Germany.

eralization. This has significant implications to hydrothermal surveys in arc environments as the seafloor expression of even large subseafloor sulfate and sulfide deposits can be comparably subtle and difficult to recognize.

KEY WORD: Tyrrhenian Sea, Aeolian Islands, volcanic arc, seamounts, hydrothermal processes and products.

RIASSUNTO - L'Arco delle isole Eolie nel Mar Tirreno sud-orientale è costituito da una catena lunga circa 180 km, composta da sette isole vulcaniche e da diversi vulcani sommersi che si estendono lungo la piattaforma continentale della Sicilia settentrionale e la Calabria occidentale.
In tre vulcani appartenenti all'Arco eoliano è stata individuata sui fondali attività idrotermale che dà luogo a depositi di solfati e solfuri, tra cui barite e solfuri di sostituzione a ~630-650 m di profondità, presso il seamount Palinuro nel settore orientale dell'Arco eoliano. Le perforazioni hanno dimostrato che tali depositi sono zonati al variare della profondità.
La parte più alta della zona mineralizzata è composta da barite e solfuri polimetallici, mentre la parte inferiore è dominata da pirite massiva con un grado marcatamente più basso di metalli comuni e preziosi. I depositi sono stati formati da fluidi idrotermali con un grado di sulfidazione intermedia, sebbene siano presenti anche escursioni ad alto e altissimo grado, indicate dalla presenza di abbondante enargite e covellite ipogenica. Il grado di sulfidazione dei minerali e la composizione isotopica dello zolfo sono indicativi di un contributo della componente volatile del magma ai fluidi idrotermali che generano i minerali. Depositi di bassa temperatura ricchi di ferro, nonché depositi di solfati e di solfuri polimetallici, si trovano anche nelle acque poco profonde di Panarea, nel settore orientale dell'arco delle isole Eolie.
Le perforazioni hanno mostrato che i depositi idrotermali subaffioranti in un'area a pockmark, originati da emissione di gas idrotermali ad una profondità di ~55-85 m, sono costituiti principalmente da anidrite e gesso con minori quantità di barite, marcasite, pirite, sfalerite, nonché alunite e caolinite.
Una emissione idrotermale a 23,5 m di profondità ha provocato la formazione di precipitati idrotermali costituiti da galena, sfalerite e barite. L'emissione si verifica anche nella zona litorale di Vulcano, dove si formano marcasite e pirite attraverso infiltrazione e sostituzione delle sabbie di spiaggia. La fuoriuscita di acque termali in acque poco profonde a Panarea e Vulcano è accompagnata dal diffuso rilascio di CO_2 che causa un'acidificazione dell'acqua di mare. L'alto flusso di gas e la composizione chimica dei fluidi suggeriscono l'esistenza di un magma in forte degassazione sotto le due isole.
Oltre ai tre sistemi idrotermali nell'arco vulcanico, attività idrotermale di bassa temperatura e fuoriuscita di acque termali sono state rilevate sulla sommità della struttura del Marsili a circa 500 m di profondità. Il ritrovamento di pirite massiva mediante dragaggio suggerisce l'esistenza di una bocca di emissione ad alta temperatura fino ad oggi non rilevata.
I punti di emissione dell'arcipelago eoliano forniscono laboratori naturali per lo studio dei processi magmatico-idrotermali che avvengono alle diverse profondità.
La constatazione che i depositi di solfati e solfuri nei vulcani dell'Arco eoliano si formano principalmente mediante processi di sostituzione nel sottofondo o sono sepolti sotto depositi sedimentari, mentre i precipitati idrotermali nelle strutture di retro-arco si formano direttamente sul fondale marino al di sopra di lave massive, evidenzia il controllo delle facies vulcaniche sulla natura della mineralizzazione. Ciò ha implicazioni significative per le indagini idrotermali in ambiente di arco vulcanico, in quanto la manifestazione sul fondale marino di depositi di solfati e di solfuri del sottofondo anche di grande entità può essere al confronto poco evidente e difficile da riconoscere.

PAROLE CHIAVE: Mare Tirreno, Isole Eolie, arco vulcanico, seamounts, processi e prodotti idrotermali.

1. - INTRODUCTION

The volcanic islands of the Aeolian archipelago in the southeastern Tyrrhenian Sea have been the focus of extensive research for over a century describing the nature and products of arc-related subaerial volcanism (MERCALLI & SILVESTRI, 1891; BERGEAT, 1899; RITTMANN, 1931; KELLER, 1980; PICHLER, 1980; CORTESE *et alii*, 1986; CLOCCHIATTI *et alii*, 1994; DELLINO & LA VOLPE, 1995; KOKELAAR & ROMAGNOLI, 1995; RIPEPE *et alii*, 2005; DE ASTIS *et alii*, 2013; FORNI *et alii*, 2013; FRANCALANCI *et alii*, 2013; LUCCHI *et alii*, 2013a-d; ROSI *et alii*, 2013). However, knowledge on the geology of the submarine portions of the volcanic islands and the adjacent submerged volcanoes is comparably limited (GABBIANELLI *et alii*, 1993; GAMBERI & MARANI, 1997; FAVALLI *et alii*, 2005; BOSMAN *et alii*, 2009; ROMAGNOLI *et alii*, 1993, 2013a,b; ROMAGNOLI, 2013). In particular, few systematic surveys for submarine hydrothermal activity have been carried out in the past, with much of the research focusing on

the more easily accessible hydrothermal systems in the littoral zone of the volcanic islands (Gamberi *et alii*, 1997; Marani *et alii*, 1997, 1999; Savelli *et alii*, 1999; Esposito *et alii*, 2006, 2018; Petersen & Monecke, 2008, 2009; Monecke *et alii*, 2009; Lupton *et alii*, 2011). The existence of deeper marine hydrothermal activity in the Tyrrhenian Sea was only confirmed in 2006 through the discovery of tubeworm colonies occurring in an area of diffuse low-temperature (<1°C above ambient) fluid discharge at a water depth of ~630-650 m below sea-level (Petersen & Monecke, 2008; Monecke *et alii*, 2009; Thiel *et alii*, 2012).

Research on the hydrothermal systems of the Aeolian archipelago is of particular interest as arc volcanism is developed on a basement of continental crust (Morelli *et alii*, 1975; Wang *et alii* 1989; Ventura *et alii*, 1999; Peccerillo *et alii*, 2006). In contrast to intraoceanic arcs formed on oceanic crust such as the well-studied Mariana and Tonga-Kermadec systems of the western Pacific (Stüben *et alii*, 1992; Wright *et alii*, 1998; de Ronde *et alii*, 2005, 2011, 2014; Lupton *et alii*, 2006, 2008; Stoffers *et alii*, 2006; Embley *et alii*, 2007; Berkenbosch *et alii*, 2012; Leybourne *et alii*, 2012a,b), volcanic island arcs such as the Aeolian archipelago have so far only been poorly surveyed (de Ronde *et alii*, 2003; Lupton *et alii*, 2011) limiting the current understanding of geodynamic controls on the nature of seafloor hydrothermal system (de Ronde *et alii*, 2003; Hannington *et alii*, 2005; Monecke *et alii*, 2014).

This contribution provides an overview of the seafloor hydrothermal systems and associated mineral deposits recognized in the Tyrrhenian Sea to date. The review focuses on three major vent sites located at the arc volcanoes of the Aeolian archipelago as well as one site of hydrothermal venting on the back-arc. The associated hydrothermal deposits are diverse in nature and occur at water depths ranging from several hundreds of meters below sea-level to the littoral zone of the volcanic islands. Research at these sites provides critical insights into seafloor hydrothermal processes occurring in island arc settings.

2. - GEOLOGICAL SETTING

The Tyrrhenian Sea is a semi-closed basin in the western Mediterranean that is bounded by mainland Italy to the northeast, Sicily to the southeast, and the islands of Corsica and Sardinia to the west. The southeastern portion of the Tyrrhenian Sea comprises the volcanoes of the Aeolian archipelago and the Marsili abyssal plain (fig. 1).

The volcanoes of the Aeolian archipelago form a tightly arcuate chain (fig. 1) that rests on a ~20 km thick continental basement (Morelli *et alii*, 1975; Wang *et alii*, 1989; Ventura *et alii*, 1999; Peccerillo *et alii*, 2006) of sedimentary and metamorphic rocks (Honnorez & Keller, 1968; Bargossi *et alii*, 1989; Clocchiatti *et alii*, 1994; Del Moro *et alii*, 1998). The Aeolian volcanic chain comprises seven major islands and several submarine seamounts extending for ~180 km parallel to the continental slope of northern Sicily and western Calabria. Volcanism in the Aeolian archipelago commenced ca. 1.3 Ma ago in the western part of the volcanic chain (Beccaluva *et alii*, 1985). Subaerial volcanic activity was restricted to the past ~500 ka. Volcanic eruptions occurred during historical times at Lipari, Stromboli, and Vulcano. Today, only Stromboli exhibits ongoing eruptive volcanism (Francalanci *et alii*, 2013; Rosi *et alii*, 2013).

The volcanoes of the Aeolian archipelago surround the Marsili abyssal plain (fig. 1), which represents a small back-arc basin formed as a consequence of roll-back of the northwestward-dipping Ionian subduction zone and migration of arc volcanism from the island of Sardinia towards the east-southeast (Barberi *et alii*, 1974; Gasparini *et alii*, 1982; Ellam *et alii*, 1989; Argnani & Savelli, 1999; Savelli, 2001). Opening of the Marsili back-arc basin was initiated close to the Pliocene-Pleistocene boundary at ~1.9 Ma (Savelli, 1988; Savelli & Schreider, 1991). The central part of the Marsili abyssal plain is occupied by the Marsili seamount (fig. 1), a prominent volcanic feature interpreted to be the superinflated spreading ridge (Marani & Trua, 2002).

Major submarine hydrothermal vent fields have so far been discovered at three of the arc volcanoes of the Aeolian archipelago (fig. 1). This includes a large polymetallic massive sulfate and sulfide occurrence at the Palinuro seamount (Minniti & Bonavia, 1984; Laschek, 1986; Puchelt & Laschek, 1987; Tufar, 1991; Marani *et alii*, 1999; Petersen & Monecke, 2009; Monecke *et alii*, 2009; Petersen *et alii*, 2014) and shallow marine polymetallic sulfates and sulfides at Panarea in the eastern sector of the Aeolian volcanic chain (Marani *et alii*, 1997; Savelli *et alii*, 1999; Becke *et alii*, 2009; Breuer, 2010; Conte & Caramanna, 2010; Petersen & Monecke, 2009; Monecke *et alii*, 2009). Pyrite and marcasite also form from thermal waters discharging in the littoral zone of Vulcano in the central sector of the Aeolian archipelago (Bernauer, 1933, 1940; Honnorez, 1969; Honnorez *et alii*, 1973; Wauschkuhn & Gröpper, 1975). Aside of these high-temperature (>100°C) vent sites and associated sulfate and sulfide deposits, Fe and Mn precipitates formed by low-

temperature fluid flow are widespread on the arc volcanoes of the Aeolian archipelago (Bonatti *et alii*, 1972; Castellarin & Sartori, 1978; Kidd & Ármannson, 1979; Morten *et alii*, 1980; Eckhardt *et alii*, 1997, Gamberi *et alii*, 1997; Marani *et alii*, 1999; Savelli *et alii*, 1999; Dekov & Savelli, 2004; Esposito *et alii*, 2018). One of the largest fields of low-temperature hydrothermal discharge and associated hydrothermal deposits is located in the summit region of the Marsili seamount (Uchupi *et alii*, 1988; Uchupi & Ballard, 1989; Savelli, 1992; Sborshchikov & Al'mukhamedov, 1992; Dekov *et alii*, 2006; Petersen & Monecke, 2008; Ligi *et alii*, 2014). This field is included in this review as a massive sulfide sample has been recovered by dredging in its immediate vicinity (Marani *et alii*, 1999) suggesting that higher temperature fluid flow may have occurred in the past at Marsili or that the corresponding vents have not yet been identified in seafloor surveys.

3. - PALINURO SEAMOUNT

The Palinuro seamount consists of eight coalesced volcanic edifices aligned along a W-trending fault system (Ghisetti & Vezzani, 1981; Boccaletti *et alii*, 1984; Tamburelli *et alii*, 2000; Rosenbaum & Lister, 2004) extending seaward off the cost of northern Calabria. To the north, Palinuro is bound by the continental slope of the Southern Apennines. The volcanic edifice faces the Marsili abyssal plain to the south (fig. 1). The Palinuro seamount extends for a length of ~75 km and has a maximum width of 35 km at the base (Monecke *et alii*, 2009; Passaro *et alii*, 2010; Pensa *et alii*, this volume).

Bathymetric surveys have shown that the Palinuro seamount consists of three distinct sectors (Fabbri *et alii*, 1973; Marani *et alii*, 1999; Monecke *et alii*, 2009; Passaro *et alii*, 2010; Ligi *et alii*, 2014). The eastern sector comprises a volcanic ridge occurring

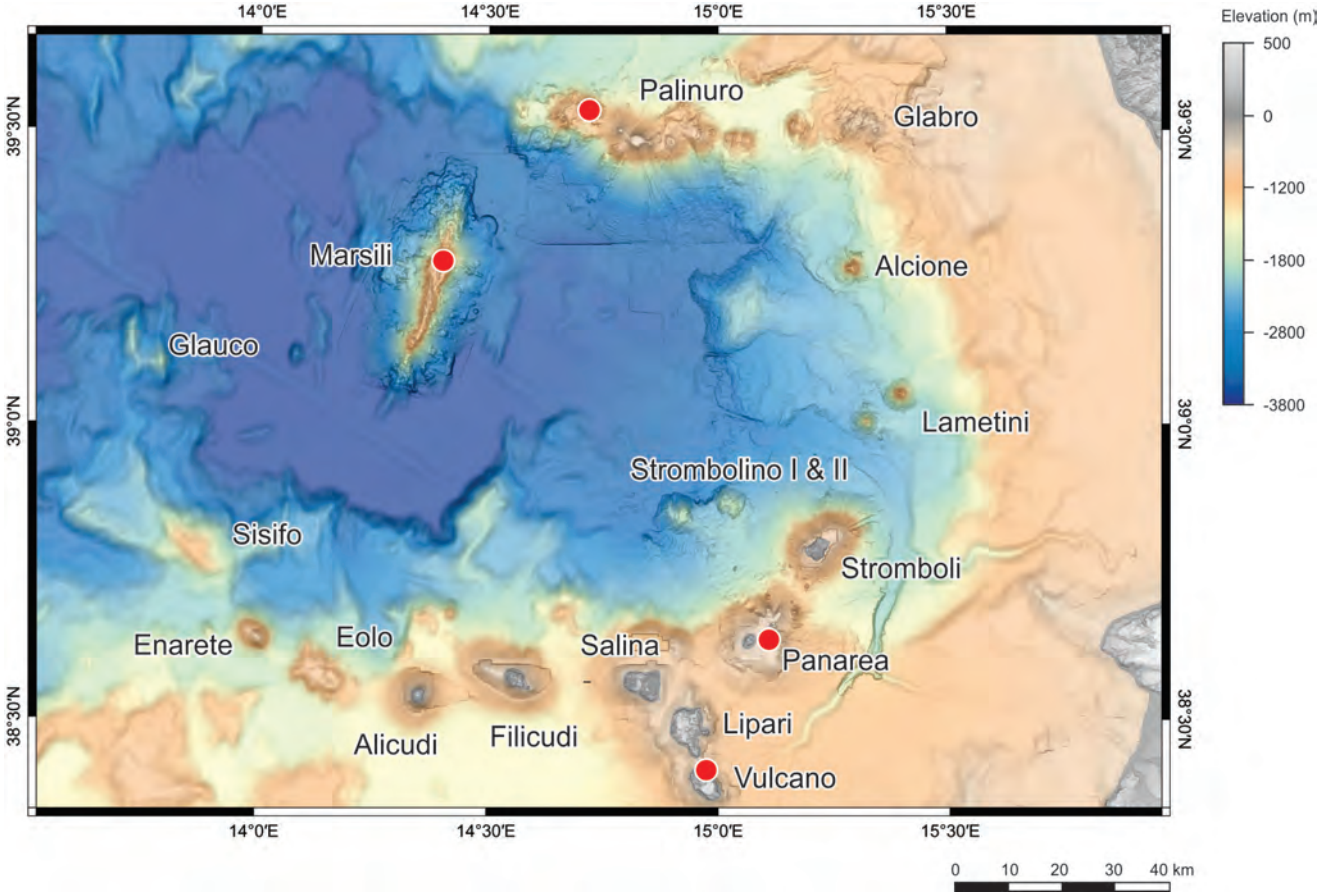

Fig. 1- Bathymetric map of the southeastern Tyrrhenian Sea showing the locations of island arc volcanoes and the Marsili back-arc basin. The red circles highlight the locations of hydrothermal fields described in the text. Shipboard bathymetric data was obtained during R/V Meteor cruises M73/2 and M86/4. Gridding was performed using a 30 m grid-cell size. To allow coverage of the entire area shown, the bathymetric data was combined with the global multi-resolution topography data of Ryan *et alii* (2009), which was gridded using a 90 m grid-cell size.

- Mappa batimetrica del Mar Tirreno sud-orientale che mostra le posizioni dei vulcani di arco insulare e il bacino di retroarco del Marsili. I cerchi rossi evidenziano le posizioni dei campi idrotermali descritti nel testo. I dati batimetrici sono stati ottenuti con ecoscandaglio di bordo durante le crociere Meteor R/V, M73/2 e M86/4. La griglia è stata eseguita utilizzando una dimensione della cella di 30 m. Per consentire la copertura dell'intera area mostrata, i dati batimetrici sono stati combinati con i dati batimetrici multi-risoluzione di Ryan et alii (2009), ottenuti da una griglia con celle di 90 m.

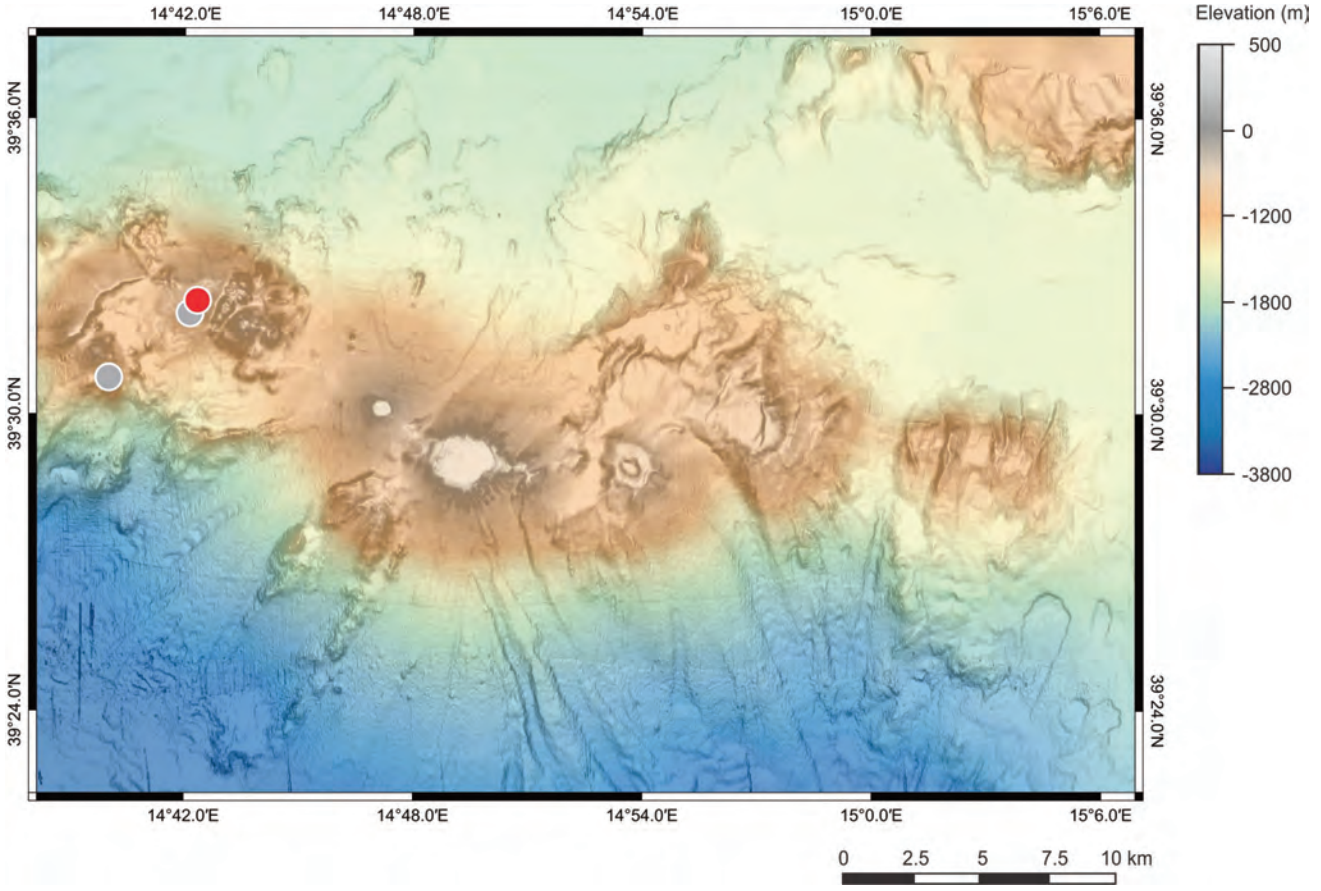

Fig. 2 - Bathymetric map of the Palinuro seamount in the southeastern Tyrrhenian Sea. The red circle highlights the location of the massive sulfide occurrence on the western summit of the volcanic edifice. The gray circles represent the locations of massive sulfide samples dredged at other locations as reported by Marani *et alii* (1999) and Petersen & Monecke (2008). Shipboard bathymetric data was obtained during R/V Meteor cruise M73/2. Gridding was performed using a 30 m grid-cell size.

- Mappa batimetrica del seamount Palinuro nel Mar Tirreno sud-orientale. Il cerchio rosso evidenzia l'ubicazione dell'area di ritrovamento dei solfuri massivi sulla vetta occidentale dell'edificio vulcanico. I cerchi grigi rappresentano le ubicazioni dei campioni di solfuri massivi dragati in altre località, come riportato da Marani et alii (1999) e Petersen & Monecke (2008). I dati batimetrici con ecoscandaglio di bordo sono stati ottenuti durante la crociera Meteor R/V, M73/2. La griglia è stata eseguita utilizzando una dimensione della cella di 30 m.

at a water depth of ~950 m (fig. 2). A semicircular headwall scarp associated with a large submarine landslide is located on the southeastern flank of this volcanic ridge. Two volcanic cones with flat circular tops are located in the central sector of the Palinuro seamount. The eastern cone has a diameter of ~2,500 m at a water depth of only 70 m, while the western cone is ~800 m in diameter and reaches a minimum water depth of 160 m (fig. 2). The flat tops of the cones probably formed as a result of erosion during the last glacial low-stand of the sea-level (Fabbri *et alii*, 1973; Passaro *et alii*, 2010). The western sector of the volcano comprises a 8-km-wide E-W-trending depression that is bound by a string of volcanic edifices to the north. These rise to a minimum depth of 500 m. A 4-km-wide semicircular depression occurs in the western part of the sector with a large volcanic edifice occurring in the southwest of the depression (fig. 2).

Basaltic to basaltic andesite samples recovered from Palinuro have a calc-alkaline affinity (Del Monte, 1972; Colantoni *et alii*, 1981) and range from 0.3 to 0.8 Ma in age (Colantoni *et alii*, 1981; Savelli, 2002). Seafloor observations have shown that large parts of the Palinuro seamount are covered by hemipelagic sediments and outcrops of volcanic rocks are relatively rare in the upper portion of the volcanic edifices. The occurrence of extensive, Fe-Mn-oxide deposits has been established by seafloor sampling and TV-guided camera surveys (Kidd & Ármannson, 1979; Minniti *et alii*, 1986; Laschek, 1986; Eckhardt *et alii*, 1997; Marani *et alii*, 1999; Dekov & Savelli, 2004).

Massive sulfides at Palinuro were discovered during systematic gravity coring performed as part of a seafloor mineral exploration campaign by Samim Ocean Inc. of the Italian National Energy Company (Minniti & Bonavia, 1984). The massive sulfide samples originated from the westernmost summit of the western sector of Palinuro. The samples showed a spongy texture and consisted of concentric layers of pyrite with small aggregates of barite.

Bismuthinite, luzonite, sphalerite, stibnite, and tennantite-tetrahedrite were recognized microscopically. The massive sulfide samples contained up to 2.24 wt % Cu and 5.80 wt % Ba. In addition, concentrations of up to 220 ppm Ag, 2,400 ppm As, 400 ppm Hg, 180 ppm Pb, 9,100 ppm Sb, and 280 ppm Zn were recorded (Minniti & Bonavia, 1984).

During R/V Sonne cruise SO41 in 1986, massive sulfides were recovered from a second site located approximately 5 km to the east of the previous discovery. This site is located in a small depression at the summit of one of the volcanic cones bordering the 8-km-wide depression in the eastern part of the western sector. The widespread staining of the fine-grained sediments covering the seafloor suggested that low-temperature hydrothermal activity occurred at the site (Laschek, 1986; Puchelt & Laschek, 1987). Massive sulfide samples recovered contained up to 1.21 wt % Cu, 28.2 wt % Zn, 14.5 wt % Pb, and 48.02 wt % Ba. Trace element concentrations of up to 460 ppm Ag, 4,900 ppm As, 7.08 ppm Au, and 6,400 ppm Hg were recorded (Puchelt & Laschek, 1987; Tufar, 1991). Tufar (1991) showed that the massive sulfides sampled are comprised of pyrite, marcasite, sphalerite, galena, and barite, with minor enargite and traces of bravoite, covellite, tennantite, and wurtzite.

Massive sulfides at both previously identified locations at the Palinuro seamount were also recovered during the R/V Urania cruise MAR98 (Marani *et alii*, 1999). Seafloor surveys at both locations were conducted in 2006 using a remotely operated vehicle onboard R/V Poseidon cruise POS340 (Petersen & Monecke, 2008). The seafloor observations showed that the eastern site discovered by Laschek (1986) and Puchelt & Laschek (1987) is covered by thick unconsolidated mud with lava only occurring as rare outcrops and subcrops (fig. 3a). In an area bounded by three low relief knolls, chimney-like structures of Fe-Mn-oxide capped by bacterial matter were observed indicating the presence of low-temperature hydrothermal activity. Locally small (<0.5 m diameter) tubeworm colonies were present that appeared to be associated with low-temperature (<1°C above ambient) fluid discharge at a water depth of ~640 m (fig. 3b; Petersen & Monecke, 2008; Monecke *et alii*, 2009; Thiel *et alii*, 2012). Seafloor observations at the western site discovered by Minniti & Bonavia (1984) also failed to identify the occurrence of sulfide chimneys or black smokers, although numerous Fe-Mn-oxide chimneys tipped by bacterial colonies were observed (Petersen & Monecke, 2008).

Drilling in the area of diffuse flow and associated tubeworm colonies was performed during R/V Meteor cruise M73/2 in 2007 using a lander-type drilling device of the British Geological Survey capable of drilling to a maximum penetration of 5 m. A total of 11 successful holes were drilled in the small depression between the low relief knolls at a water depth of 610 to 650 m (Monecke *et alii*, 2009; Petersen *et alii*, 2014). A total of 13.5 m of core were recovered, including a 4.84-m-long section of continuous massive and semimassive sulfate and sulfide (fig. 3c). Seafloor observations made during drilling showed that unconsolidated mud covers much of the seafloor in the area investigated, which is consistent with the rapid drilling progress made in the upper parts of the holes. The sediment cover appears to increase in thickness towards the south, southwest, and northwest. Drilling showed that the subseafloor sulfate and sulfide occurrence is at least 50 by 35 m in size. All drill holes ended in massive to semimassive sulfate and sulfide suggesting that the mineralized zone is of substantial thickness. As the unconsolidated sediments overlying the massive and semimassive sulfates and sulfides could not be recovered, TV-guided grab sampling was also performed onboard R/V Meteor cruise M73/2. Recovered material included abundant banded silica-sulfide-barite samples, Fe-Mn oxides, and fine-grained indurated sediments and volcaniclastic rocks (Monecke *et alii*, 2009; Petersen *et alii*, 2014). Native sulfur made up a substantial amount of the material recovered (fig. 3d). Unconsolidated mud recovered by TV-guided sampling was warm when brought on deck, with maximum temperatures of 60°C being recorded (Petersen *et alii*, 2014).

The massive and semimassive sulfate and sulfides recovered are generally fine-grained with grain sizes typically being <100 μm. The porosity of the drill core is highly variable ranging from <10 % in massive pyrite to >30 % in vuggy barite-sulfide. Reflected light microscopy shows that pyrite is the most abundant ore mineral (Petersen *et alii*, 2014). Pyrite forms recrystallized euhedral grains or occurs as colloform banded aggregates. Textural evidence suggests that the pyrite in the drill core formed paragenetically early and was overprinted by polymetallic main-stage mineralization (fig. 4a). In polymetallic assemblages, pyrite is typically intergrown with euhedral barite. Chalcopyrite and tetrahedrite were found to be the principal Cu minerals in drill core and form part of the polymetallic main-stage mineralization (fig. 4b,c). Some of the larger tetrahedrite aggregates contain inclusions of famatinite and rare cinnabar. Fracture filling and overgrowth by fine-grained enargite is present. In addition to these minerals, sphalerite, galena, and Pb-Sb-As sulfosalts including bournonite-seligmannite as well as semseyite are common in the polymetallic main-stage mineralization forming euhedral crystals or fine-

grained disseminated grains. Sphalerite is translucent in thin section, which is consistent with the low to intermediate Fe contents measured by electron microprobe analyses (average of 0.80 wt % Fe, n = 311). In some drill holes, a distinct sulfide assemblage was recognized that is characterized by the presence of euhedral covellite intergrown with enargite and galena (fig. 4d). The principal gangue minerals in the drill core samples are barite, opal-A, and native sulfur (PETERSEN *et alii*, 2014). Geochemical analyses of 36 drill core intervals revealed that the massive to semimassive sulfate and sulfides at Palinuro contain on average 1.6 wt % Cu, 2.8 wt % Zn, 1.9 wt % Pb, 0.39 ppm Au, and 130 ppm Ag (PETERSEN *et alii*, 2014). The samples analyzed show an anomalous enrichment in As, Hg, and Sb (tab. 1). In general, the top of the mineralized zone showed higher base and precious metal grades than the pyrite-dominated lower portion of the mineralized zone (PETERSEN *et alii*, 2014).

Following the successful identification of subseafloor massive and semimassive sulfates and sulfides, Palinuro has been revisited several times as a test site for seafloor experiments and, in particular, testing of geophysical equipment. A range of geophysical investigations were conducted onboard R/V Urania cruises TIR10 in 2010 and MAVA2011 in 2011. The research showed that the area around

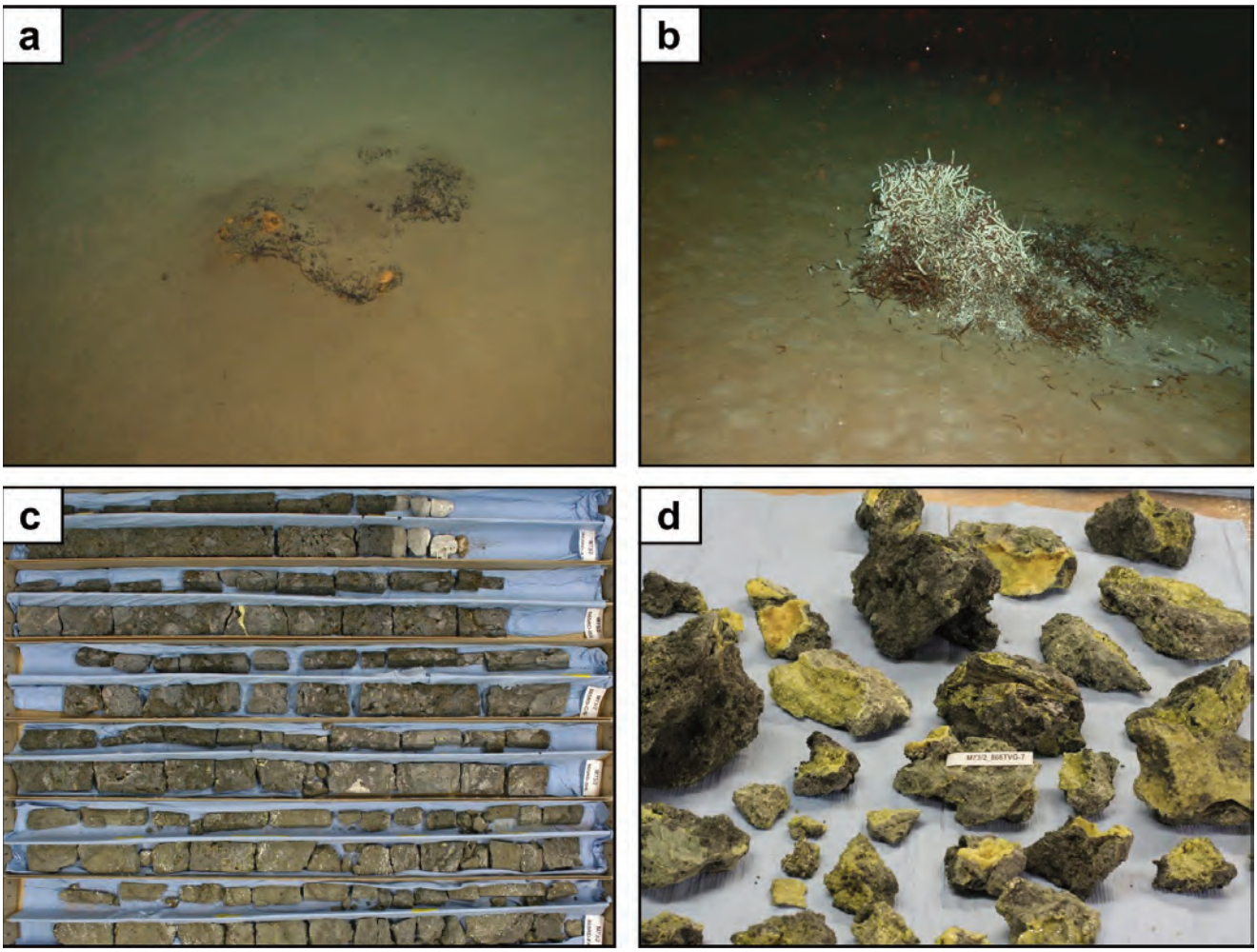

Fig. 3 - Seafloor images and hydrothermal precipitates sampled at the hydrothermal vent field at the Palinuro seamount in the southeastern Tyrrhenian Sea. a) Subcrop of lava or hydrothermal precipitates topped by small Fe-Mn chimneys. The surrounding seafloor is covered by unconsolidated mud. Field of view is ~2 m. Station 741ROV of R/V Poseidon cruise POS340. b) Vestimentiferan tubeworm colony associated with minor low-temperature fluid discharge. Station 743ROV of R/V Poseidon cruise POS340. c) Drill core consisting of massive to semimassive sulfate and sulfide. The stratigraphic top is at the upper RIGHT of the image and the stratigraphic bottom is at the lower left. Note the bleached top contact marking the transition from massive sulfide to overlying mud. Station 865RD of R/V Meteor cruise M73/2. The drill hole penetrated to a depth of 4.85 m. d) Sulfur-rich samples recovered by TV-guided grab sampling. Station 866TVG of R/V Meteor cruise M73/2.

- Immagini del fondale marino e dei precipitati idrotermali campionati presso il campo di emissione idrotermale del seamount Palinuro nel Mar Tirreno sud-orientale. a) Subaffioramento di lava o di precipitati idrotermali, sormontato da piccoli camini ferro-manganesiferi. Il fondo marino circostante è coperto da fango non consolidato. Il campo visivo è ~2 m. Stazione 741ROV della crociera Poseidon R/V, POS340. b) Colonia di gallerie di Vestimentifera associata a una minore fuoriuscita di fluido a bassa temperatura. Stazione 743ROV della crociera Poseidon R/V, POS340. c) Carotaggio costituito da solfati e solfuri massivi e semimassivi. Il top stratigrafico è in alto a destra dell'immagine e la base stratigrafica è in basso a sinistra. Notare il contatto superiore sbiancato che segna la transizione dal solfuro massivo al fango sovrastante. Stazione 865RD della crociera Meteor R/V, M73/2. Il carotiere è penetrato fino a una profondità di 4,85 m. d) Campioni ricchi di zolfo recuperati mediante prelievo con telecamera filo-guidata. Stazione 866TVG della crociera Meteor R/V, M73/2.

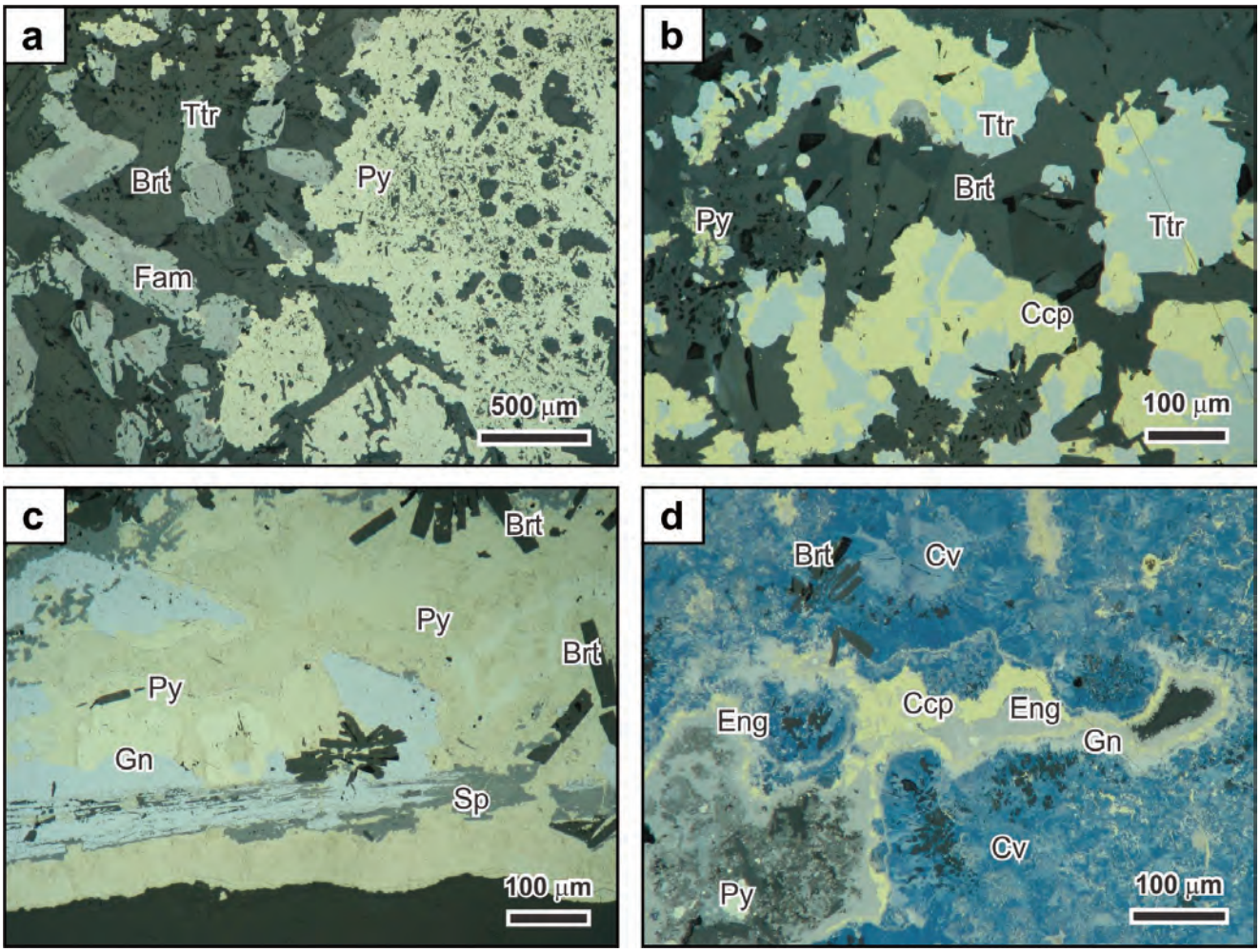

Fig. 4 - Reflected light microscopy images of massive sulfate and sulfide samples obtained by drilling at the hydrothermal vent field at the Palinuro seamount in the southeastern Tyrrhenian Sea. a) Massive pyrite overgrown by main-stage barite, tetrahedrite, and famatinite. Sample 851RD072–076. b) Main stage chalcopyrite and tetrahedrite intergrown with barite and minor pyrite. Sample 932RD018–023. c) Late colloform pyrite intergrown with galena and sphalerite. The sulfide minerals overgrow euhedral barite crystals. Multiple generations of pyrite can be identified in reflected light. Sample 932RD066–070. d) Aggregate of covellite overgrown by enargite and chalcopyrite. The covellite is intergrown with enargite and galena on a submicron scale. The outer boundary of the enargite is diffuse and irregular in shape (lower left) and shows an association with globular pyrite. Sample 853RD002–006. Drilling was performed during R/V Meteor cruise M73/2 using a lander-type drilling device of the British Geological Survey. Brt = barite, Ccp = chalcopyrite, Cv = covellite, Eng = enargite, Fam = famatinite, Gn = galena, Py = pyrite, Sp = sphalerite, Ttr = tetrahedrite.

- Immagini al microscopio in luce riflessa di campioni di solfati e solfuri massivi acquisiti mediante perforazione nel campo di emissione idrotermale presso il seamount Palinuro nel Mar Tirreno sud-orientale. a) Barite, tetraedrite e famatinite accresciute nella fase principale di precipitazione su pirite massiva. Campione 851RD072-076. b) Intercrescita da fase principale di precipitazione di calcopirite e tetraedrite con barite e subordinata pirite. Campione 932RD018-023. c) Pirite tardiva colloidale intercresciuta con galena e sfalerite. I minerali di solfuro crescono su cristalli di barite euedrale. Più generazioni di pirite possono essere identificate a luce riflessa. Campione 932RD066-070. d) Sovracrescita di enargite e calcopirite su aggregato di covellite. La covellite è intercresciuta con enargite e galena a una scala inferiore al micron. Il limite esterno dell'enargite è di forma diffusa e irregolare (in basso a sinistra) e mostra un'associazione con pirite globulare. Campione 853RD002-006. La perforazione è stata eseguita durante la crociera Meteor R/V, M73/2 utilizzando un dispositivo di perforazione di tipo lander del British Geological Survey. Brt=barite, Ccp=calcopirite, Cv=covellite, Eng=enargite, Fam=famatinite, Gn=galena, Py=pirite, Sp=sfalerite, Ttr=tetraedrite.

the drill site is characterized by a broad magnetic low that likely is linked to intense alteration of the footwall volcanic rocks (Caratori Tontini *et alii*, 2014; Ligi *et alii*, 2014). A water column survey onboard R/V Urania in 2007 revealed a notable δ^3He anomaly (~2 % above background) above the drill site. Additional anomalies were detected at the eastern slope of the central sector and in the far eastern end of the volcano (Lupton *et alii*, 2011). Gravity coring and sampling of the vestimentiferan tubeworm colonies using a remotely operated vehicle were conducted onboard R/V Poseidon cruise POS412 in 2011 (Thiel *et alii*, 2012). The drill site was also revisited during R/V Meteor cruise M86/4 in early 2012. Extensive gravity coring was conducted to characterize the unconsolidated mud overlying the mineralized zone. Sediment temperatures of 26.8° to 58°C were measured after recovery on deck. At an ambient seawater bottom temperature of 13.2°C, this confirmed that hydrothermal activity is ongoing at Palinuro (Petersen, 2014a). An autonomous underwater vehicle was deployed during R/V Poseidon cruise POS442 in late 2012 to conduct sidescan sonar and subbottom profiling surveys and to collect

Tab. 1 - *Ranges of major and trace element concentrations of sulfate and sulfide samples (n = 36) recovered by drilling at the Palinuro seamount in southeastern Tyrrhenian Sea. The samples were obtained during R/V Meteor cruise M73/2.*
- Intervalli di concentrazione degli elementi maggiori e in traccia di campioni (n=36) di solfati e solfuri recuperati mediante carotaggio presso il seamount Palinuro nel Mar Tirreno sud-orientale. Icampioni sono stati ottenuti durante la crociera Meteor R/V, M73/2.

Element	Concentration range
As	0.03 - 1.51 wt %
Cu	0.02 - 5.58 wt %
Pb	0.03 - 7.12 wt %
Sb	0.01 - 2.23 wt %
Zn	0.03 - 26.70 wt %
Ag	<2 - 925 ppm
Au	0.02 - 3.38 ppm
Bi	<2 - 1,390 ppm
Cd	1 - 1,070 ppm
Co	<1 - 52 ppm
Hg	11 - 2,920 ppm
Mo	20 - 200 ppm
Ni	<1 - 45 ppm
V	1 - 58 ppm

seafloor images as well as magnetic and water column data (Petersen, 2014b; Szitkar *et alii*, 2015). Electromagnetic experiments and visual seafloor surveys were conducted onboard R/V Poseidon cruise POS483 in 2015 (Jegen, 2015; Safipour *et alii*, 2018). Seismic investigations were carried out onboard R/V Poseidon cruise POS484/2 in 2015 (Bialas, 2015). In addition to electromagnetic and electrochemical experiments (Safipour *et alii*, 2017, 2018), a heat flow probe was deployed during R/V Poseidon cruise POS509 in 2017 to measure the temperature distribution in the area surrounded by the three low-relief knolls. Temperature measurements were conducted at 10 to 220 cm depth within the unconsolidated mud at 33 locations. A maximum temperature of 49°C was noted. A total of 23 stations yielded thermal conductivity data. The data collected was used to construct a thermal gradient map, which clearly illustrates that the area of hydrothermal activity at Palinuro is much larger than suggested by drilling in 2007 (Hölz, 2017).

4. - PANAREA ISLAND

Panarea is the smallest volcanic island of the Aeolian archipelago (fig. 1). The island rises from the western sector of a 56 km^2, near-circular submarine platform that occurs at a water depth of 120 m. This platform is the flat, eroded summit of a large submarine stratovolcano that is over 1,500 m in height with a basal diameter of 17.5 km (fig. 5a; Gabbianelli *et alii*, 1990; Favalli *et alii*, 2005). Panarea is primarily composed of high- K basaltic -andesite to rhyolite lavas interbedded with pyroclastic deposits. The subaerial portion of the volcanic edifice is as old as 149±5 ka (Calanchi *et alii*, 1999). The rhyolite dome of the islet of Basiluzzo located to the east of the main island has been dated at 54±8 to 46± 8 ka (Gabbianelli *et alii*, 1990; Dolfi *et alii*, 2007; Bigazzi *et alii*, 2008). Some of the youngest products of effusive volcanism at Panarea yielded an age of 20±2 ka (Dolfi *et alii*, 2007).

A large field of shallow-water hydrothermal activity is located approximately 3 km to the east of Panarea, on the eastern sector of the near-circular submarine platform of the volcano (fig. 5a). In this area, gas and thermal water venting occurs at water depths of approximately 5 to 35 m on top of a shallow rise of the 2.3 km^2 seafloor surrounding the islets of Panarelli, Lisca Bianca, Bottaro, Lisca Nera, and Dattilo (Italiano & Nuccio, 1991; Calanchi *et alii*, 1995; Esposito *et alii*, 2006; Capaccioni *et alii*, 2007; Tassi *et alii*, 2009; Caramanna *et alii*, 2010). Quiescent degassing in the area surrounding the central islets has been ongoing since early historic times (Italiano & Nuccio, 1991; Calanchi *et alii*, 1995; Caliro *et alii*, 2004; Esposito *et alii*, 2006; Aliani *et alii*, 2010) at an average flux of ~16 tonnes per day (Italiano & Nuccio, 1991). Venting of thermal waters on the seafloor supports a diverse community of extremophile bacteria (Gugliandolo *et alii*, 2006, 2012, 2015; Maugeri *et alii*, 2009; Lentini *et alii*, 2014).

Bathymetric mapping in the area of the central islets revealed the presence of numerous explosion

craters on the seafloor suggesting that the quiescent CO_2 discharge is punctuated by short periods of violent gas discharge (ESPOSITO *et alii*, 2006; MONECKE *et alii*, 2012). Gas eruptions at Panarea have been documented in 126 BC (ESPOSITO *et alii*, 2006) as well as 1815 and 1865 (SMYTH, 1824; MERCALLI, 1883). A large hydrothermal gas eruption occurred in the night between November 2nd and 3rd, 2002, marking the end of a prolonged seismotectonic paroxysmal period in southern Italy (ESPOSITO *et alii*, 2006; HEINICKE *et alii*, 2009). In the early morning, fishermen observed vigorous gas bubbling at the sea surface between Lisca Bianca, Bottaro, and Lisca Nera (fig. 5b). Thousands of fish had perished, presumably as a result of a measurable drop of the seawater ph to 5.6-5.7 (CALIRO *et alii*, 2004; CHIODINI *et alii*, 2006). A strong smell of H_2S was detectable as far away as Panarea. A multibeam bathymetric survey of the seafloor revealed that the explosion resulted in the formation of an elliptical crater that was 35 m long, 25 m wide, and over 10 m deep (ANZIDEI *et alii*, 2005; ESPOSITO *et alii*, 2006; ALIANI *et alii*, 2010). Intense gas venting lasted until mid 2003 (ALIANI *et alii*, 2010; MONECKE *et alii*, 2012). During the hydrothermal crisis, an estimated 50,000 tonnes of CO_2 were released (MONECKE *et alii*, 2012). The presence of magmatic volatile species (SO_2, HCl, and HF) in the gas emission is suggestive for a magmatic input at depth (CALIRO *et alii*, 2004; CHIODINI *et alii*, 2006; CAPACCIONI *et alii*, 2007; TASSI *et alii*, 2009).

Following the gas eruption in November 2002, significant research ensued in the area of anomalous degassing around the central islets to determine the seafloor geology and the composition of the gases emitted (CALIRO *et alii*, 2004; ANZIDEI *et alii*, 2005; CARACAUSI *et alii*, 2005; CHIODINI *et alii*, 2006; ESPOSITO *et alii*, 2006; CAPACCIONI *et alii*, 2007; TASSI *et alii*, 2009, 2014; FABRIS *et alii*, 2010). During scuba diving surveys in November 2002, a vent site emitting dark colored smoke was discovered in 23.5 m water depth northwest of Lisca Nera and east of Dattilo (fig. 5b; ESPOSITO *et alii*, 2006; CONTE & CARAMANNA, 2010). Thermal water emission at the site occurred at a temperature of ~30°C

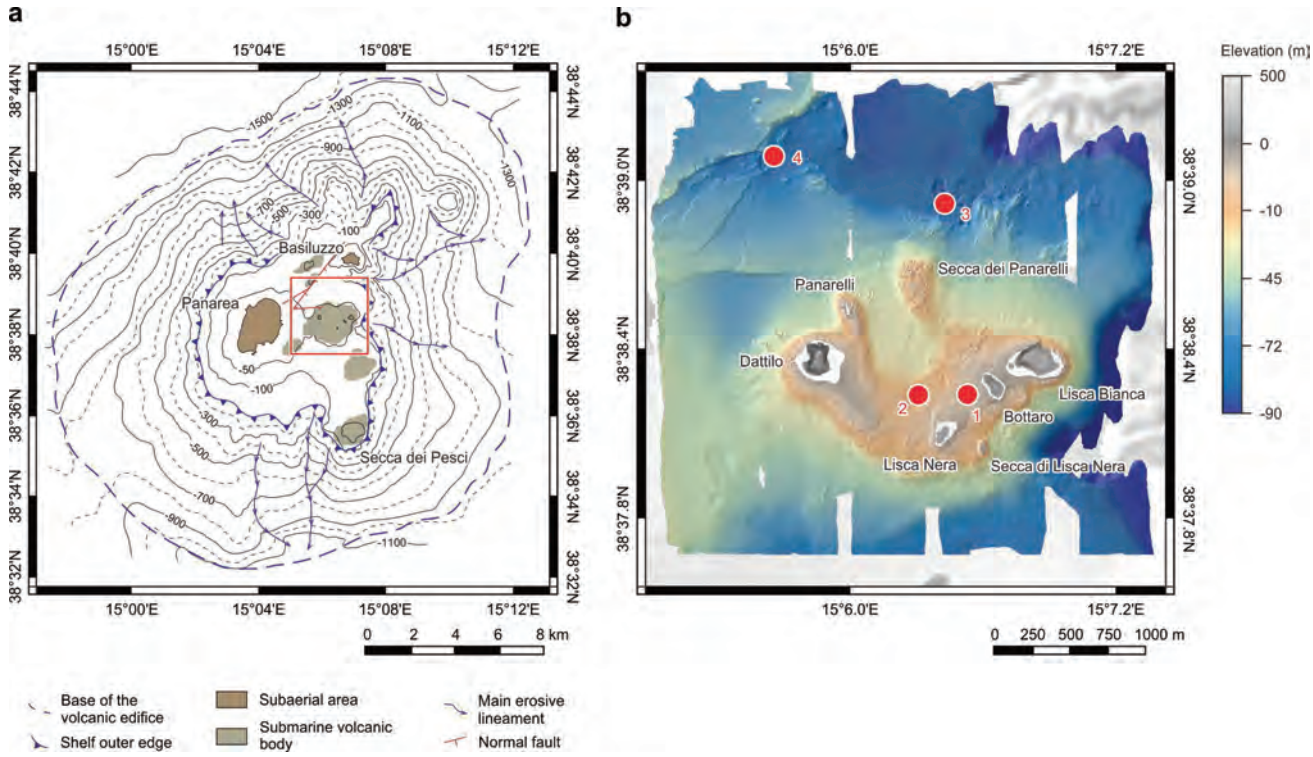

Fig. 5 - Location of shallow marine fumaroles at Panarea island in the southeastern Tyrrhenian Sea. a) Bathymetric map of the Panarea seamount (modified from LUCCHI *et alii*, 2013d). The red outline highlights the location of the detailed shaded bathymetric map given on the right. b) Bathymetric map of the area surrounding the central islets located east of the main island. The red circles highlight the locations of the vent fields known to be associated with sulfate and sulfide precipitates. Bathymetric data are from ESPOSITO *et alii* (2006) and was gridded at a 1-m grid size. Digital elevation model of islets from TARQUINI & NANNIPIERI (2017). 1 = Location of the 2002 hydrothermal eruption, 2= Hydrothermal vent field that precipitated sulfates and polymetallic sulfides at a water depth of 23.5 m. 3 = Hydrothermal vent field located in the NW-trending trough to the northeast of the Secca dei Panarelli, 4 = Area of intense CO_2 venting described by Linke (2014) and of Fe-oxide chimneys and mounds described by ESPOSITO *et alii* (2018).

- Posizione delle fumarole sottomarine poco profonde presso l'isola di Panarea nel Mar Tirreno sud-orientale. a) Mappa batimetrica del seamount Panarea (modificata da LUCCHI et alii, 2013d). Il contorno rosso evidenzia la posizione della mappa batimetrica ombreggiata dettagliata sulla destra. b) Mappa batimetrica dell'area che circonda gli isolotti centrali situati a est dell'isola principale. I cerchi rossi evidenziano le posizioni dei campi di emissione noti per essere associati a precipitati di solfuri e solfati. I dati batimetrici sono di ESPOSITO et alii (2006) e sono stati elaborati su una griglia con cella di 1 m. Modello di elevazione digitale degli isolotti da TARQUINI & NANNIPIERI (2017). 1 = Posizione dell'eruzione idrotermale del 2002, 2 = Campo di emissione idrotermale che ha generato solfati e solfuri polimetallici, a una profondità di 23,5 m. 3 = Campo di emissione idrotermale situato nel canale allineato NO a nord-est della Secca dei Panarelli, 4 = Area di intensa emissione di CO_2 descritta da LINKE (2014) e camini e mound di ossidi di Fe descritti da ESPOSITO et alii (2018).

(Voltattorni *et alii*, 2009). Black smoke was still observed in March 2003 (Conte & Caramanna, 2010). Temperatures of the discharging thermal waters increased and temperatures of 110-137°C were recorded between 2003 and 2008 (Becke *et alii*, 2009; Tassi *et alii*, 2009; Voltattorni *et alii*, 2009; Conte & Caramanna, 2010). Since 2005, fluid emission from the site was dominated by gas bubbling and the discharge of clear thermal waters (Conte & Caramanna, 2010). The thermal waters contain high Hg contents (Bagnato *et alii*, 2017).

The site of the black smoke emission is located in a 26 by 24 m large and 5 m deep subcircular depression formed during a past gas explosion (Esposito *et alii*, 2006; Becke *et alii*, 2009). Emission occurred from a small subangular outcrop of gravel- to cobble-sized volcanic material cemented by black hydrothermal precipitates (Conte & Caramanna, 2010). Recovered samples from the site include volcanic clasts coated by thin (<2 mm) layers of hydrothermal precipitates. Some of the surface coatings consist predominately of Fe-Mn-oxides, with bulk samples containing up to 45.2 wt % MnO. In addition, sulfide-rich coatings were identified. These contain up to 37.3 wt % Zn, 13.20 wt % Pb, 7.38 wt % Ba, and 1.35 wt % Sr (Becke *et alii*, 2009). Scanning electron microscopy on these precipitates revealed the presence of abundant opal-A in addition to barite, galena, and minor sphalerite (Becke *et alii*, 2009; Conte & Caramanna, 2010). Barite occurs as up to 100 μm large platy crystals whereas galena forms small octahedral crystals (fig. 6). Sphalerite commonly forms small globular aggregates. In addition to these phases, the rare Pb-As

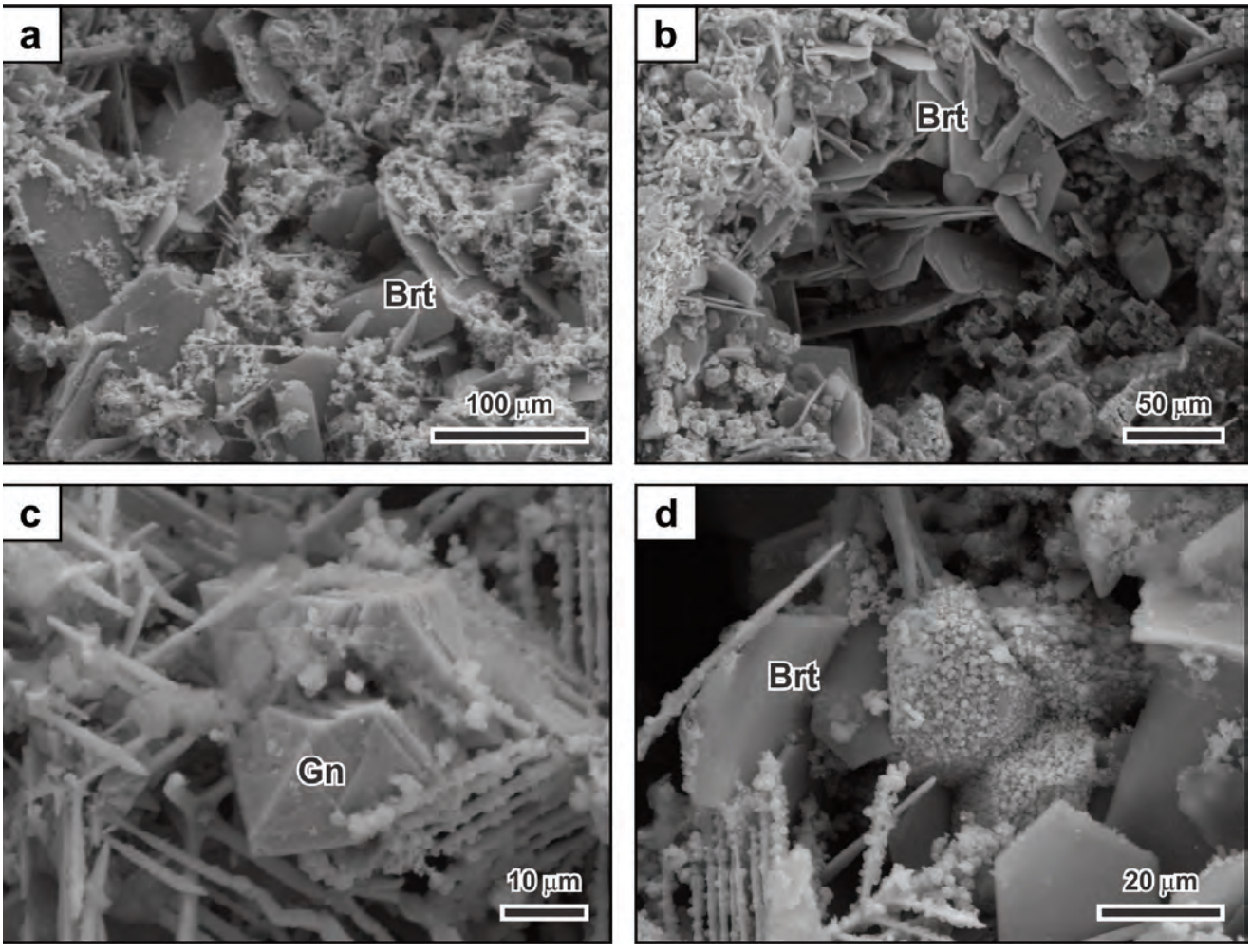

Fig. 6 - Topography contrast scanning electron microscope images of sulfate and sulfide precipitates from Panarea Island in southeastern Tyrrhenian Sea. The samples were recovered at a water depth of 23.5 m northwest of Lisca Nera and east of Dattilo. a) Platy barite coated by fine-grained sulfate and sulfide phases. b) Intergrown platy barite crystals. c) High-magnification image of a galena octahedron. d) High-magnification image of platy barite coated by fine-grained sulfate and sulfide phases. Brt =barite, Gn = galena.

- Immagini al microscopio elettronico a scansione del contrasto di rilievo di precipitati di solfati e solfuri dall'Isola di Panarea nel Mar Tirreno sud-orientale. I campioni sono stati recuperati ad una profondità di 23,5 m a nord-ovest di Lisca Nera e ad est di Dattilo. a) Barite tabulare rivestita da fasi di solfati e solfuri a grana fine . b) Cristalli di barite tabulari intercresciuti. c) Immagine ad alto ingrandimento di un ottaedro di galena. d) Immagine ad alto ingrandimento di barite tabulare rivestita da fasi di solfato e solfuro a grana fine. Brt = barite, Gn = galena.

sulfosalt gratonite was identified (CONTE & CARAMANNA, 2010).

In addition to the area between the central islets, widespread hydrothermal venting has been recorded to the north between the Secca dei Panarelli and Basiluzzo (fig. 5b; MARANI *et alii*, 1997; SAVELLI *et alii*, 1999; MONECKE *et alii*, 2009, 2012; SCHMIDT *et alii*, 2015). Seafloor bathymetric investigations show that the seafloor in a relatively small area northeast of the Secca dei Panarelli is pockmarked by circular gas eruption craters occurring at a water depth of up to 85 m (ESPOSITO *et alii*, 2006; MONECKE *et alii*, 2012). The diameter of the craters ranges from 5 to 50 m, with the largest crater having a diameter of 120 m. The craters are of low relief with only 0.5-4 m from floor to rim. The crater walls range from steep to gentle. Some of the explosion craters are surrounded by low-relief deposits or mounds at their rims that are steep on the inside, but gently dip outward from the craters. Composite craters and clusters of overlapping depressions are present, including a NW-trending trough that occurs at a water depth of ~80 m (MONECKE *et alii*, 2012). Seafloor observations using a remotely operated vehicle on-

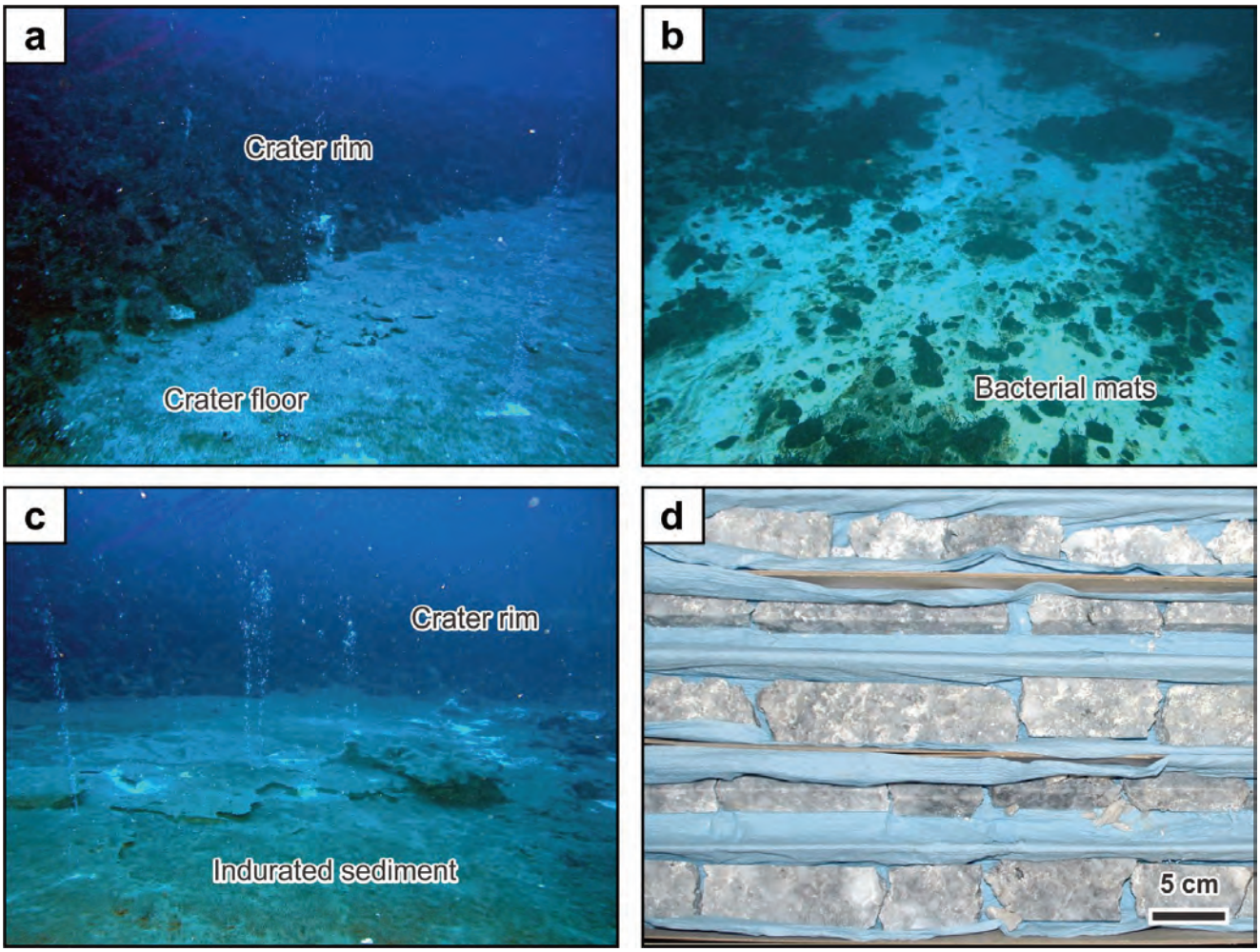

Fig. 7 - Seafloor images and drill core from the hydrothermal vent field located northeast of the Secca dei Panarelli at Panarea in southeastern Tyrrhenian Sea. a) Inside of a gas explosion crater that is surrounded by a steep-walled rim composed of rounded cobbles and boulders. The flat crater floor is covered by sandy to gravelly sediment. Local gas bubbling is observed. Field of view is ~5 m. Image from MONECKE *et alii* (2012). b) Floor of a gas explosion crater that is littered by volcanic clasts. Bacterial mats cover the seafloor in areas of diffuse thermal water discharge. Field of view is ~2 m. Image from MONECKE *et alii* (2012). c) Site of gas bubbling and thermal water discharge at the floor of an explosion crater. Gas venting occurs from small chimney-like structures and cracks in the indurated sediment. The indurated sediment is cemented by native sulfur, which is also present in the small chimney-like structures. The crater wall can be seen in the background. Field of view is about 5 m. Image from MONECKE *et alii* (2012). d) Drill core consisting of massive anhydrite and gypsum with minor polymetallic sulfides. Drilling of the hole at 61 m water depth was performed during R/V Meteor cruise M73/2 using a lander-type drilling device of the British Geological Survey (station RD881). The drill hole penetrated to a depth of 5 m. A total of 2.89 m of core were recovered.

- Immagini del fondale marino e carotaggio proveniente dal campo di emissione idrotermale situato a nord-est della Secca dei Panarelli a Panarea nel Mar Tirreno sud-orientale. a) Interno di un cratere di esplosione di gas, circondato da un bordo a pareti ripide composto da ciottoli e massi arrotondati. Il fondo piatto del cratere è coperto da sedimenti da sabbiosi a ghiaiosi. Si osservano localmente bolle di gas. Il campo visivo è ~5 m. Immagine da MONECKE et alii (2012). b) Fondo di un cratere di esplosione di gas, disseminato di clasti vulcanici. Tappeti batterici coprono il fondale marino in aree a rilascio diffuso di acqua termale. Il campo visivo è ~2 m. Immagine da MONECKE et alii (2012). c) Area di degassamento e rilascio di acqua termale sul fondo di un cratere di esplosione. L'emissione del gas proviene da piccole strutture tipo camini e da fratture nel sedimento cementato da zolfo nativo, presente anche nelle piccole strutture a camino. Sullo sfondo è visibile la parete del cratere. Il campo visivo è di circa 5 m. Immagine da MONECKE et alii (2012). d) Carota costituita da anidrite massiva, gesso e in minor quantità da solfuri polimetallici. Il carotaggio, a 61 m di profondità, è stata eseguito durante la crociera Meteor R/V, M73/2 utilizzando un carotiere di tipo lander del British Geological Survey (stazione RD881). La carota ha raggiunto una profondità di 5 m. Sono stati recuperati in totale 2,89 m di carotaggio.

board R/V Poseidon in 2006 revealed that vigorous gas venting is widespread, indicating ongoing geothermal activity. In addition to the gas venting, diffuse discharge of thermal waters was observed. Discharge sites are commonly marked by the occurrence of white bacterial mats (fig. 7a-c; PETERSEN & MONECKE, 2008; MONECKE *et alii*, 2009, 2012). Using echosounding, high quality water column data was collected during R/V Meteor cruise M86/4 in 2012 along an E-W transect north of the Secca dei Panarelli and south of Basiluzzo (PETERSEN, 2014b). Large flares of CO_2 emitted from the seafloor can be observed along much of the transect (fig. 8). Similar CO_2 discharge was also observed onboard R/V Urania cruise U10/2011 in 2011 and R/V Poseidon cruise POS469 in 2014 (fig. 5b; MCGINNIS *et alii*, 2011; LINKE, 2014).

In 1995, box-coring to a maximum depth of 60 cm yielded the first evidence for the presence of sulfide deposits in the NW-trending trough northeast of the Secca dei Panarelli (fig. 5b; GAMBERI *et alii*, 1997; MARANI *et alii*, 1997; SAVELLI *et alii*, 1999). In the cores recovered, sulfide minerals occurred within argillic-altered host rocks. Two decimeter-sized polymetallic massive sulfide fragments were recovered. These contained up to 16.9 wt % Zn, 4.8 wt % Pb, and 11.6 wt % Ba. Optical microscopy and scanning electron microscopy revealed the presence of galena, sphalerite, pyrite and marcasite, as well as abundant barite (GAMBERI *et alii*, 1997; MARANI *et alii*, 1997; SAVELLI *et alii*, 1999).

The area in which the sulfides were recovered through dredging was mapped in detail using a remotely operated vehicle onboard R/V Poseidon cruise POS340 in 2006. Seafloor mapping showed the presence of widespread subcrops that appeared to be composed of gray to white hydrothermal precipitates (PETERSEN & MONECKE, 2008). During R/V Meteor cruise M73/2 in 2007 (PETERSEN & MONECKE, 2009; MONECKE *et alii*, 2009), a lander-type drilling system of the British Geological Survey was employed, capable of drilling to a maximum penetration of 5 m. The use of a seabed camera system allowed targeting and positioning of the rig on the seafloor prior to the commencement of the drilling operation. In total, eight holes recovering massive anhydrite-gypsum were drilled at water depths of 55-85 m, yielding 7.84 m of core at an overall recovery of 20.6 %. The longest continuous core recovered was 2.89 m in length (fig. 7d).

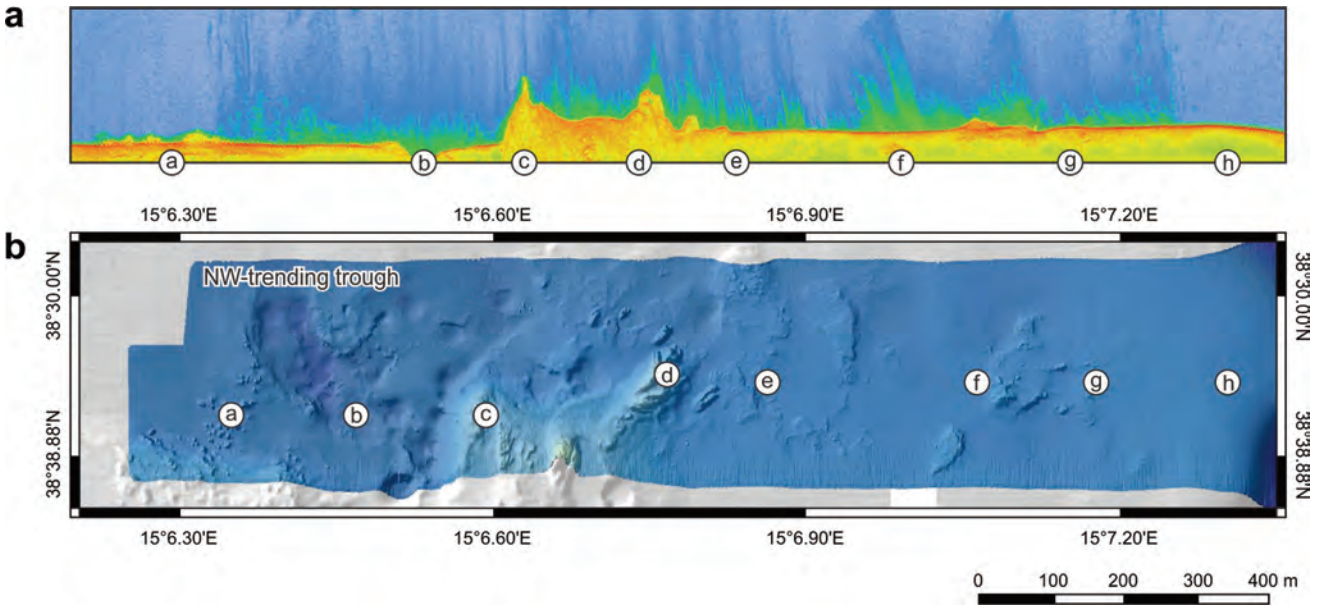

Fig. 8 - Water column and bathymetric data collected along an E-W transect between the Secca dei Panarelli and Basiluzzo near Panarea Island in the southeastern Tyrrhenian Sea. a) Water column data collected using the EM710 echosounding system of R/V Meteor during cruise M86/4 (stations 293MB and 297MB). To obtain high quality data, the ship cruised at a speed of only one knot. The figure shows the flares of CO_2 released from the seafloor. The image is not geometrically correct and intentionally distorted to show as many water column features as possible. Locations on the distorted water column image correspond to those shown in the bathymetric map. b) High-resolution bathymetric map of the E-W transect. Massive sulfate and sulfide was recovered from the NW-trending trough in the western part of the transect. Bathymetric data were collected during R/V Meteor cruise M86/4 (stations 293MB and 297MB) and are gridded at a 1-m grid size. The gray-shaded background topography is from ESPOSITO *et alii* (2006) gridded at 1-m resolution.

- Dati della colonna d'acqua e dati batimetrici raccolti lungo un transetto E-O tra la Secca dei Panarelli e Basiluzzo presso l'Isola di Panarea nel Mar Tirreno sud-orientale. a). Dati della colonna d'acqua raccolti utilizzando il sistema di ecoscandaglio EM710 del Meteor R/V durante la crociera M86/4 (stazioni 293 MB e 297 MB). Per ottenere dati di alta qualità, la nave ha viaggiato a una velocità di un solo nodo. La figura mostra le venute di CO_2 sul fondale marino. L'immagine non è geometricamente corretta ed è distorta intenzionalmente per mostrare più caratteristiche possibili della colonna d'acqua. Le posizioni della colonna d'acqua nell'immagine distorta corrispondono a quelle mostrate nella mappa batimetrica. b. Mappa batimetrica ad alta risoluzione del transetto E-O. I solfati e i solfuri massivi sono stati recuperati dalla depressione con asse NO nella parte occidentale del transetto. I dati batimetrici sono stati raccolti durante la crociera Meteor R/V, M86/4 (stazioni 293 MB e 297 MB) e sono stati elaborati su una griglia con cella di 1 m. La topografia ombreggiata dello sfondo è tratta da ESPOSITO et alii (2006) con una risoluzione di 1 m.

Half core samples were used for whole-rock mineralogical and geochemical analyses. Quantitative mineralogical analysis was performed by X-ray diffraction using the Rietveld method as described in MONECKE *et alii* (2001). The results of these investigations showed that the subcropping hydrothermal precipitates are composed of 81.2-99.6 wt % anhydrite plus gypsum. The relative proportions of both sulfate minerals vary substantially between the different drill holes. Gypsum occurs at the highest concentrations close to the seafloor. The abundance of gypsum decreases with depth whereas the amount of anhydrite increases down-hole. Thin section microscopy shows that the gypsum replaces the anhydrite (fig. 9a,b). Alunite occurs in concentrations of up to 9.8 wt % forming small platy crystals commonly occurring with pyrite (fig. 9b). Kaolinite is the most abundant clay mineral occurring in concentrations of up to 7.2 wt % in three of the drill holes, while smectite is the principal clay mineral in the samples from the other five drill holes. Kaolinite is the only clay mineral occurring in drill core sections containing alunite. Barite (up to 2.2 wt %), marcasite (up to 3.9 wt %), pyrite (up to 7.7 wt %), and sphalerite (up to 1.5 wt %) are present in some of the core samples. Pyrite and sphalerite commonly form small euhedral crystals surrounded by a matrix consisting of anhydrite and gypsum (fig. 9c,d). Mi-

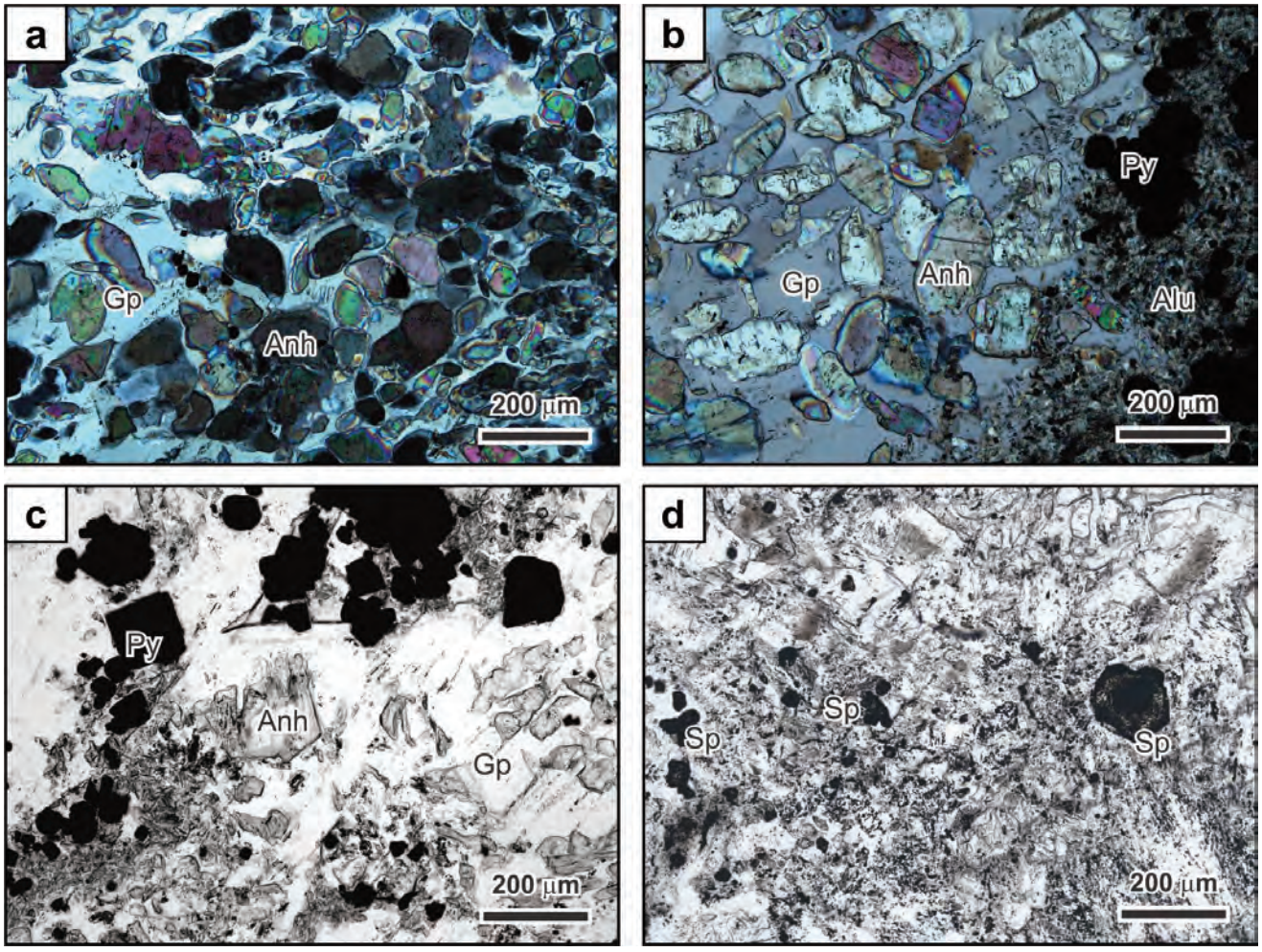

Fig. 9 - Transmitted light thin section images of sulfate and sulfide samples obtained by drilling at the hydrothermal vent field located northeast of the Secca dei Panarelli at Panarea in southeastern Tyrrhenian Sea. a) Intergrowth of gypsum and anhydrite. The anhydrite occurs as relic grains within the gypsum matrix. The high birefringence of anhydrite gives it much higher order polarizing colors than gypsum. Sample 881RD257–261. Crossed-polarized light image. b) Intergrowth of anhydrite and gypsum. Pyrite occurs within a band containing abundant alunite. Sample 881RD257–261. Crossed-polarized light image. c) Clusters of euhedral pyrite occurring in a matrix of anhydrite and gypsum. Sample 881RD257–261. Plane polarized light image. d) Fine-grained disseminated euhedral sphalerite occurring in a matrix of anhydrite and gypsum. Sample 880RD036–039. Plane polarized light image. Drilling was performed during R/V Meteor cruise M73/2 using a lander-type drilling device of the British Geological Survey. Alu = alunite, Anh = anhydrite, Gp = gypsum, Py = pyrite, Sp = sphalerite. - *Immagini di sezioni sottili a luce trasmessa di campioni di solfati e solfuri ottenuti mediante carotaggio nel campo di emissione idrotermale situato a nord-est della Secca dei Panarelli a Panarea, nel Mar Tirreno sud-orientale. a) Intercrescita di gesso e anidrite. L'anidrite è presente come granuli relitti all'interno della matrice di gesso. L'alta birifrangenza dell'anidrite le conferisce colori di polarizzazione di ordine molto superiore rispetto al gesso. Campione 881RD257-261. Immagine a nicol incrociati. b) Intercrescita di anidrite e gesso. La pirite è presente all'interno di una fascia contenente abbondante alunite. Campione 881RD257-261. Immagine a nicol incrociati. c) Cluster di pirite euedrale in matrice di anidrite e gesso. Campione 881RD257-261. Immagine a nicol paralleli. d) Sfalerite euedrale a grana fine disseminata in una matrice di anidrite e gesso. Campione 880RD036-039. Immagine a nicol paralleli. La perforazione è stata eseguita durante la crociera Meteor R/V, M73/2 utilizzando un carotiere di tipo lander del British Geological Survey. Alu = alunite, Anh = anidrite, Gp = gesso, Py = pirite, Sp = sfalerite.*

croprobe analysis showed that the pyrite at Panarea can be enriched in As, with spot analyses ranging up to 0.33 wt % As (Breuer, 2010). The sphalerite is translucent in thin section and has a low Fe content of 0.06-0.91 wt % (n=13; Breuer, 2010). Whole-rock geochemical analyses confirmed that the core samples are primarily composed of calcium sulfate. The samples are enriched in Ag, As, Ba, Cd, Hg, Pb, Sb, and Zn (tab. 2).

Low-temperature hydrothermal activity has been recorded further west during R/V Poseidon cruise POS340 in 2006. Seafloor surveying using a remotely operated vehicle (station 754ROV) revealed the abundant presence of small Fe-rich chimneys northeast of Panarelli on the footwall side of a major NE-trending fault (fig. 5b; Petersen & Monecke, 2008). The chimneys were still hydrothermally active as suggested by the presence of bacterial matter around chimney orifices and the occurrence of shimmering water. More recent mapping of the area established the occurrence of a large area of low-temperature hydrothermal venting along the NE-trending fault (Esposito *et alii*, 2018). Mineralogical and geochemical analyses indicate that these chimneys are largely composed of Fe-oxyhydroxides (>80 wt % Fe_2O_3) with minor silica (6.8 to 9.2 wt % SiO_2) and Na_2O (2.2 to 2.8 wt %). Elevated concentrations of As, Mo, Pb, Sr, and V were recorded (Esposito *et alii*, 2018).

5. - VULCANO ISLAND

Vulcano is the southernmost of the seven volcanic islands of the Aeolian archipelago. The island is the exposed portion of a large volcanic edifice that rises from the 1,200-m-deep seafloor to a maximum height of 499 m above sea-level at Monte Aria (fig. 10a). Vulcano is located immediately south of Lipari from which it is separated by a shallow-water (~50 m below sea-level) saddle (Favalli *et alii*, 2005). Together with Lipari and Salina, Vulcano forms a NNW-trending volcanic belt, the location of which is controlled by the Tindari-Letojanni fault system (Ventura, 1994; Mazzuoli *et alii*, 1995; Ventura *et alii*, 1999; Chiarabba *et alii*, 2004).

Volcanological evidence and historical observations suggest that Vulcano is one of the most active volcanoes in the Mediterranean (De Astis *et alii*, 2013). Volcanic activity at the island commenced ~127 ka ago (Solìgo *et alii*, 2000; De Astis *et alii*, 2013). Over the past 5.5 ka, volcanic activity took place at the Fossa cone in the central sector of the island (Gillot, 1987; De Astis *et alii*, 2013). The edifice, dominantly composed of pyroclastic deposits with subordinate lava flows, rises 391 m above the

Tab. 2 - *Ranges of major and trace element concentrations of sulfate and sulfide samples (n = 21) recovered by drilling at the hydrothermal vent field located northeast of the Secca dei Panarelli off Panarea Island in southeastern Tyrrhenian Sea. The samples were obtained during R/V Meteor cruiseM73/2.*
- Intervalli di concentrazione degli elementi maggiori ed in traccia di campioni (n = 21) di solfati e solfuri recuperati mediante carotaggio nel campo di emissione idrotermale situato a nord-est della Secca dei Panarelli a largo dell'Isola di Panarea, nel Mar Tirreno sud-orientale. I campioni sono stati ottenuti durante la crociera Meteor R/V, M73/2.

Element	Concentration range
SiO_2	0.52 - 6.09 wt %
TiO_2	0.01 - 0.12 wt %
Al_2O_3	0.61 - 4.53 wt %
Fe_2O_3	0.21 - 8.07 wt %
MnO	<0.01 - 2.28 wt %
MgO	<0.01 - 0.89 wt %
CaO	27.58 - 36.32 wt %
Na_2O	<0.01 - 0.30 wt %
K_2O	<0.01 - 0.53 wt %
P_2O_5	<0.01 - 0.02 wt %
LOI	11.48 - 23.13 wt %
S	17.50 - 23.10 wt %
Ag	<0.5 - 8.6 ppm
As	6 - 274 ppm
Au	<1 ppb
Ba	5 - 10,240 ppm
Bi	<2 ppm
Cd	<0.5 - 20.9 ppm
Co	1.1 - 15 ppm
Cu	2.0 - 62 ppm
Hg	37 - 8,790 ppb
Mo	<2 - 18 ppm
Ni	<1 - 19 ppm
Pb	<5 - 2,690 ppm
Sb	0.7 - 70.8 ppm
Sr	1,018 - 1,987 ppm
V	9 - 55 ppm
Zn	1 - 8,640 ppm

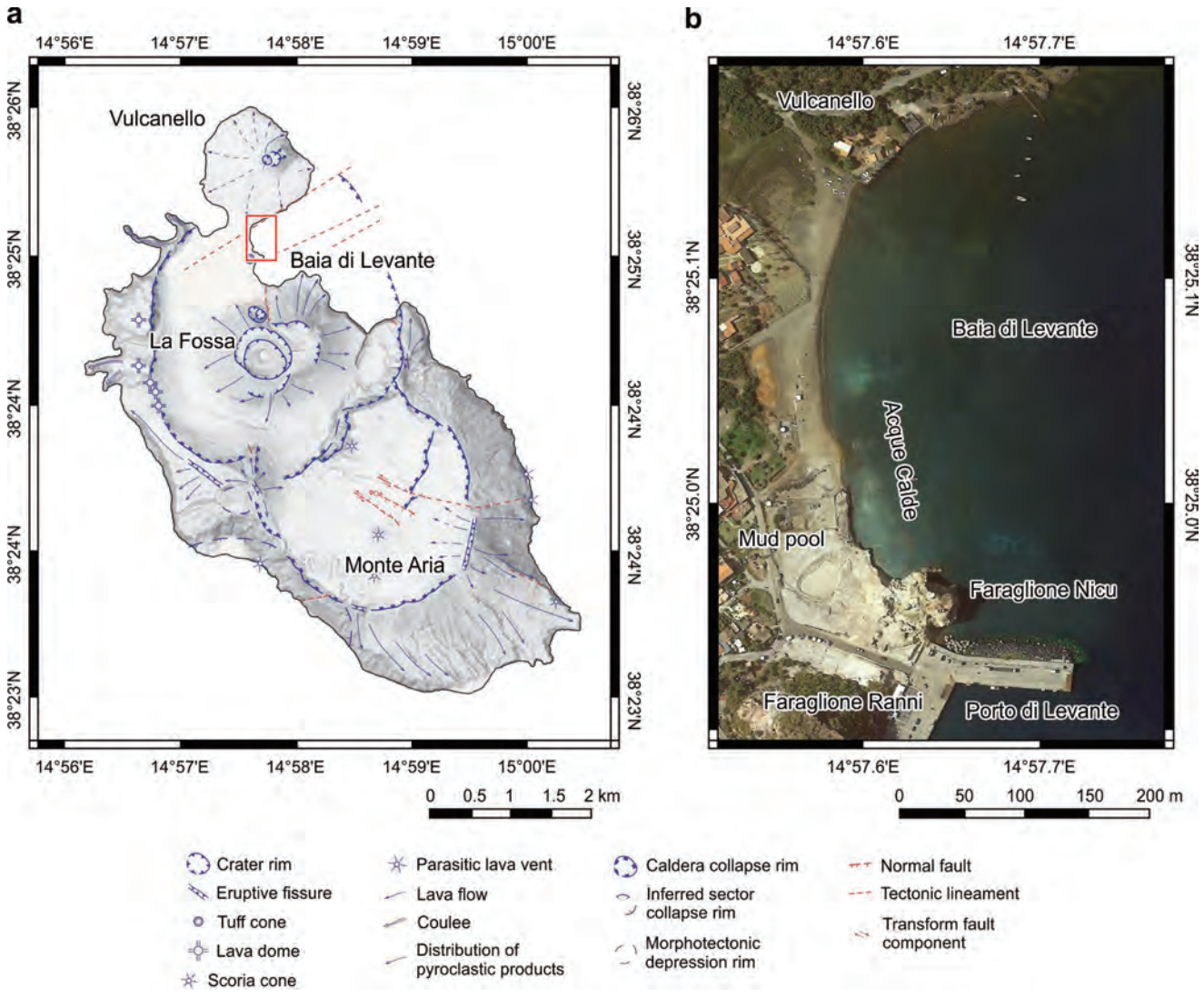

Fig. 10 - Location of shallow marine fumaroles at Vulcano Island in the southeastern Tyrrhenian Sea. a) Map of Vulcano showing the location of the Baia di Levante (modified from De Astis *et alii*, 2013). The red outline gives the location of the detailed map of the Baia di Levante given on the right. b) Satellite image of the zone of shallow marine venting in the Baia di Levante. The image shows the location of the Faraglione volcanic cone and mud pools. The Acque Calde area is located north of Faraglione Nicu.

- Posizione delle fumarole marine a bassa profondità presso l'Isola di Vulcano, nel Mar Tirreno sud-orientale. a) Mappa di Vulcano che mostra la posizione della Baia di Levante (modificata da De Astis et alii, 2013). Il contorno rosso indica la posizione della mappa dettagliata della Baia di Levante sulla destra. b) Immagine satellitare della zona di emissione marina a bassa profondità nella Baia di Levante. L'immagine mostra la posizione del cono vulcanico del Faraglione e delle pozze di fango. L'area di Acque Calde si trova a nord di Faraglione Nicu.

sea-level and has a basal diameter of ~1 km (fig. 10a). Its last eruptive event, characterized by intense explosive eruptions, lasted from August 1888 until March 1890 (Mercalli & Silvestri, 1891). Since this eruption, high-temperature (up to 690°C) fumarolic activity has persisted along the northern rim of the Fossa cone (Cioni & D'Amore, 1984; Chiodini *et alii*, 1993, 1995; Capasso *et alii*, 1997, 1999; Diliberto, 2017).

Low-temperature fumarolic activity (up to 100°C) at Vulcano occurs in the Baia di Levante on the eastern side of the isthmus connecting the northern part of Vulcano with Vulcanello (fig. 10b, 11; Honnorez *et alii*, 1973; Wauschkuhn & Gröpper, 1975; Chiodini *et alii*, 1995; Capasso *et alii*, 1997, 1999; Capaccioni *et alii*, 2001; Svensson *et alii*, 2004). The low-temperature fumarolic activity has destroyed much of the vegetation along the shoreline from Faraglione Nicu in the south to Vulcanello in the north, creating a large barren field parallel to the shore line (Honnorez *et alii*, 1973; Wauschkuhn & Gröpper, 1975). Geochemical analyses have shown that the fumaroles of the Baia di Levante have a high CO_2 content, measurable concentrations of H_2S and CH_4, but are low in CO and lack SO_2 (Honnorez, 1969; Honnorez *et alii*, 1973; Chiodini *et alii*, 1995; Capaccioni *et alii*, 2001; Amend *et alii*, 2003). The total CO_2 flux in the beach area is estimated to be ~5.0 tonnes per day (Inguaggiato *et alii*, 2012). The

discharge sites of the beach fumaroles are characterized by the presence of abundant hydrated sulfate minerals, which formed as a result of fluid-rock interaction and sublimation from the fumarolic vapors (fig. 11b,c; GARAVELLI *et alii*, 1996). Geothermal wells drilled in the Baia di Levante area show that the volcanic rocks in the subsurface are characterized by intense advanced argillic alteration. Frequent anhydrite and barite veins were encountered to a depth of 150 m (FULIGNATI *et alii*, 1996).

In addition to the shoreline fumaroles, hydrothermal discharge is also present in the shallow waters of the bay where thermal water discharge and intense CO_2 bubbling and streaming can be observed (fig. 11d; BERNAUER, 1933, 1940; HONNOREZ *et alii*, 1973; VALETTE, 1973; WAUSCHKUHN & GRÖPPER, 1975; GARAVELLI *et alii*, 1996; SEDWICK & STÜBEN, 1996). Under water, fumarolic activity is concentrated in the southern portion of the bay near Faraglione Nicu at a water depth of up to 18 m (WAUSCHKUHN & GRÖPPER, 1975). In the northern part of the bay, hydrothermal activity is restricted to a narrow strip along the beach, referred to as Acque Calde (fig. 10b; HONNOREZ, 1969; GARAVELLI *et alii*, 1996), where hydrothermal discharge occurs at a water depth of 1-2 m (WAUSCHKUHN & GRÖPPER, 1975). Submarine venting sustains a diverse thermophilic and hyperthermophilic microbial community (AMEND *et alii*, 2003; TOR *et alii*, 2003; RUSCH *et alii*, 2005). The total amount of CO_2 discharged from submerged vents is estimated to be ~3.6 tonnes per day (INGUAGGIATO *et alii*, 2012).

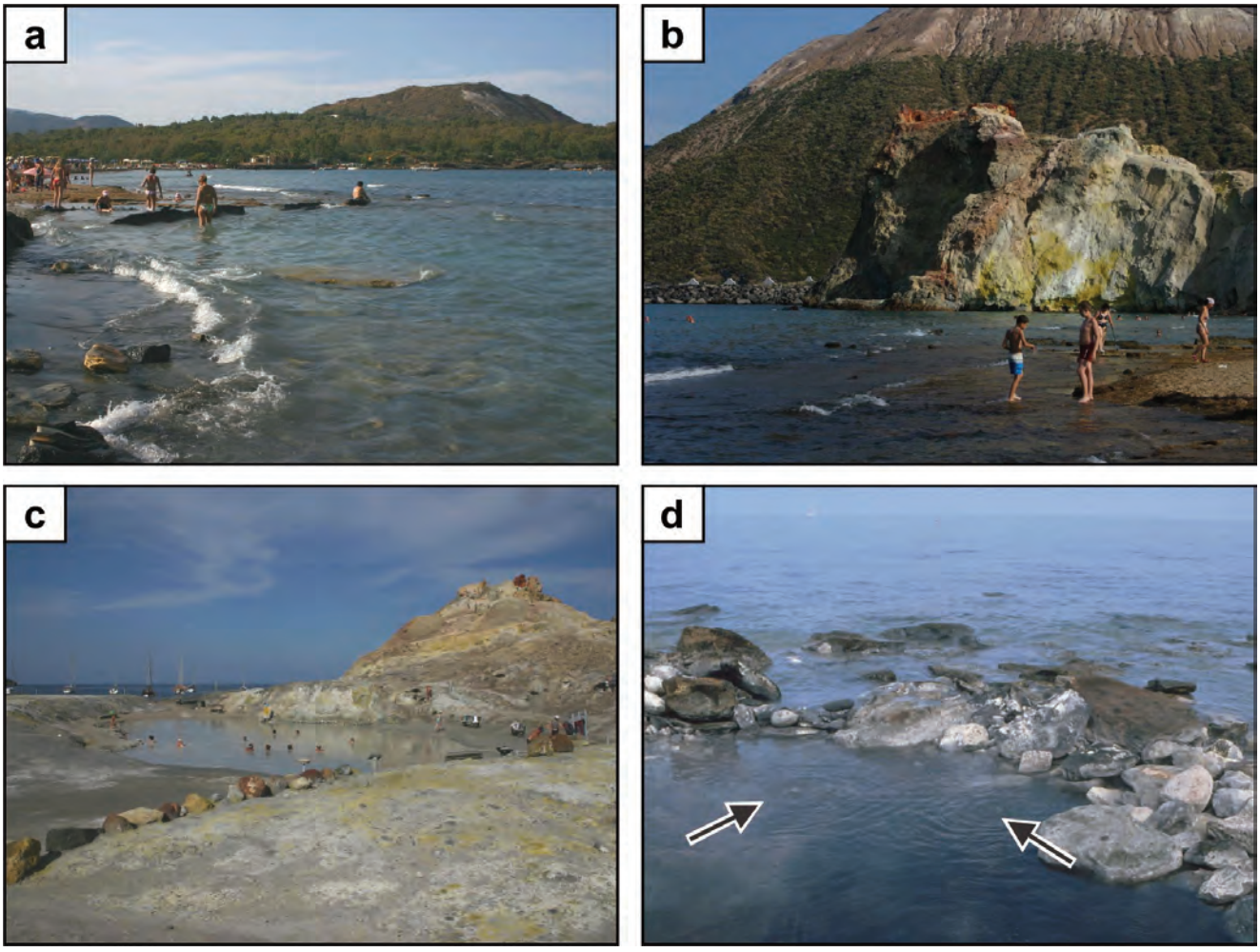

Fig. 11 - Shallow marine fumaroles in the Baia di Levante on Vulcano Island in the southeastern Tyrrhenian Sea. a) Baia di Levante looking north towards Vulcanello. Hydrothermal venting occurs along the beach and in the shallow waters of the bay. b) Baia di Levante looking south towards Faraglione Nicu. Hydrothermal venting occurs in the shallow waters of the bay and in greater water depth around Faraglione Nicu. Note the intense alteration of the exposed volcanic rocks and the sulfur sublimates. The La Fossa cone can be seen in the background. c) Mud pool located northwest of Faraglione Nicu. Note intense steam-heated alteration and the presence of sulfur sublimates. d) Submerged fumaroles in the Baia di Levante. The CO_2 bubbling can be seen between the rocks (arrows).

- Fumarole di mare basso nella Baia di Levante presso l'Isola di Vulcano nel Mar Tirreno sud-orientale. a) Vista verso nord dalla Baia di Levante in direzione di Vulcanello. L'emissione idrotermale avviene lungo la spiaggia e nelle acque basse della baia. b) Vista verso sud dalla Baia di Levante in direzione di Faraglione Nicu. L'emissione idrotermale avviene nelle acque poco profonde della baia e a maggiore profondità intorno a Faraglione Nicu. Notare l'intensa alterazione delle rocce vulcaniche esposte e i sublimati di zolfo. Il cono La Fossa è visibile sullo sfondo. c) Pozza di fango situata a nord-ovest di Faraglione Nicu. Notare l'intensa alterazione idrotermale e la presenza di sublimati di zolfo. d) Fumarole sommerse nella Baia di Levante. Le bolle di CO_2 sono visibili tra le rocce (frecce).

The gas discharge results in an acidification of the surface seawaters to ph values as low as 5.7, which is significantly lower than normal Mediterranean seawater values of 8.1-8.2 (WAUSCHKUHN & GRÖPPER, 1975; SEDWICK & STÜBEN, 1996; BOATTA *et alii*, 2013).

Fumarolic activity in the Baia di Levante results in the formation of pyrite and marcasite both on land and in the shallow waters of the bay (BERNAUER, 1933, 1940; HONNOREZ, 1969; HONNOREZ *et alii*, 1973; WAUSCHKUHN & GRÖPPER, 1975). Sulfide abundance is highest in the shallow subsurface in the littoral zone (20-40 cm below the water-sediment interface) with sulfide abundances reaching up to ~30 % (BERNAUER, 1940; HONNOREZ, 1969; HONNOREZ *et alii*, 1973; WAUSCHKUHN & GRÖPPER, 1975). Although most of the fumarolic activity is restricted to the beach area of the Baia di Levante, dredging onboard R/V Mechelen in 1968 showed that pyrite and marcasite are present in the heavy mineral fraction of sediments recovered as deep as 700 m in the eastern part of the bay (HONNOREZ *et alii*, 1973).

Pyrite and marcasite cement the sand grains in the surface sediments of the Baia di Levante (fig. 12a) or occur finely disseminated throughout the matrix surrounding the volcanic detritus (fig. 12b). The sulfide minerals also line and infill fractures in the sand grains of volcanic provenance, including perlitic fractures, and infill vesicles in originally vesicular sand grains. Pyrite and marcasite frequently re-

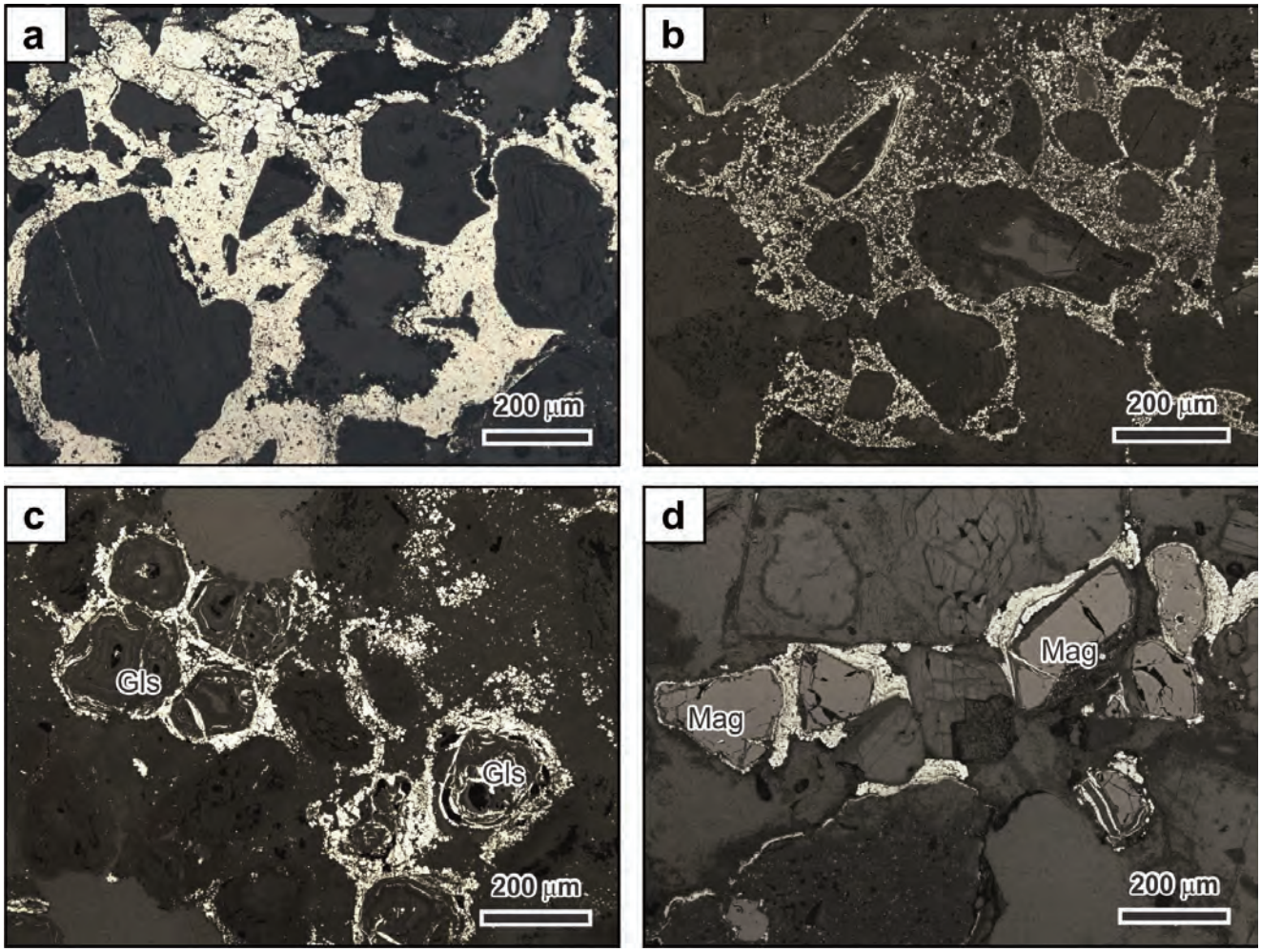

Fig. 12 - Reflected light thin section images of pyrite and marcasite occurring in surface samples dredged in the Baia di Levante on Vulcano Island in the south-eastern Tyrrhenian Sea. a) Pyrite and marcasite forming a cement around sand grains of volcanic provenance. Sample E68/27. b) Pyrite and marcasite occurring as fine-grained aggregates and euhedral grains in the matrix surrounding volcanic detritus. Sample E68/28. c) Fine-grained pyrite and marcasite cementing and replacing volcanic glass. The sulfide minerals rim the glass fragments, occur along fractures and locally replace the glass. Sample E68/26B. d) Grains of magnetite cemented by fine-grained pyrite and marcasite. The sulfide minerals rim the magnetite and occur along fractures. The magnetite shows only minor evidence for corrosion along the grain boundaries. Sample E68/25. Gls = volcanic glass, Mag = magnetite. The samples were collected by J. HONNOREZ.

- Immagini in sezione sottile a luce riflessa di pirite e marcasite presenti in campioni superficiali dragati nella Baia di Levante presso l'Isola di Vulcano, nel Mar Tirreno sud-orientale. a) Pirite e marcasite che formano un cemento attorno ai granuli di sabbia di provenienza vulcanica. Campione E68/27. b) Pirite e marcasite che si presentano come aggregati a grana fine e granuli euedrali nella matrice che circonda il detrito vulcanico. Campione E68/28. c) Pirite e marcasite a grana fine che cementano e sostituiscono il vetro vulcanico. I solfuri bordano i frammenti di vetro; si formano lungo le fratture e sostituiscono il vetro vulcanico. Campione E68/26B. d) Granuli di magnetite cementati da pirite e marcasite a grana fine. I solfuri bordano la magnetite e sono presenti lungo le fratture. La magnetite mostra solo minori evidenze di corrosione lungo i margini dei granuli. Campione E68/25. Gl = vetro vulcanico, Mag =magnetite. I campioni sono stati raccolti da J. HONNOREZ.

place volcanic glass (fig. 12c), but do not typically alter minerals such as titanomagnetite and pyroxene (fig. 12d). The sulfide minerals occur as colloform aggregates or small (<10 μm) euhedral crystals. Most of the small euhedral crystals are anisotropic in crossed polarized light, suggesting they are composed of marcasite (fig. 12). In addition, sulfide framboids ranging up to 50 μm in size are present in the volcanic sands (HONNOREZ, 1969; WAUSCHKUHN & GRÖPPER, 1975). Geochemical analysis shows that bulk sediment samples dredged from the seafloor of the Baia di Levante can be highly enriched in Fe_2O_3. The samples also show anomalously high As, Ba, Cu, and Zn values. Low concentrations of gold (<1 ppm) were detected in some samples (tab. 3).

6. - MARSILI SEAMOUNT

The Marsili seamount is located in the central part of the ocean-floored ~8,000 km^2 Marsili back-arc basin (fig. 1). The volcano, interpreted to represent the superinflated spreading ridge (MARANI & TRUA, 2002), rises ~3,500 m from the surrounding basement to a minimum water depth of 489 m. The seamount has an elongated shape and has a length of ~50 km from NNE to SSW, with a width of up to 30 km (fig. 13). It is characterized by a narrow, segmented summit ridge that stretched for about 20 km along the main axis of the volcano. The summit region, which occurs mainly above the 1,000 m isobath, is generated by the linear alignment of elongated ca. 200 m high volcanic cones and the occurrence of contiguous cones forming narrow cone ridges. A large number of parasitic or flank cones that have a basal diameter of ~1 km and range up to 350 m in height are located along the northern and western margins of the seamount (SBORSHCHIKOV *et alii*, 1989; SAVELLI, 1992; SBORSHCHIKOV & AL'MUKHAMEDOV, 1992; SAVELLI & GASPAROTTO, 1994; MARANI & TRUA, 2002; TRUA *et alii*, 2002). The basin to the east and west of the Marsili edifice exhibits several steep fault scarps that have throws in the order of 200 to 400 m and are generally parallel to the trend of the summit region of Marsili (MARANI & TRUA, 2002; TRUA *et alii*, 2002). Geomagnetic surveys of the Marsili back-arc basin suggest that volcanism at Marsili occurred largely during the past 780 ka of the Brunhes polarity chron (BRUSILOVSKIY & GORODNITSKIY, 1990; FAGGION *et alii*, 1995; NICOLOSI *et alii*, 2006). Lavas collected from the summit of the Marsili seamount yielded K/Ar ages of <0.2 Ma (SELLI *et alii*, 1977). Volcanism may have taken place as recent as 5 ka ago (IEZZI *et alii*, 2014).

Tab. 3 - *Ranges of major and trace element concentrations in samples (n = 20) containing pyrite and marcasite obtained by dredging in the Baia di Levante on Vulcano. The samples werecollected by J. HONNOREZ.*
- Intervalli di concentrazione degli elementi maggiori ed in traccia in campioni (n = 20) contenenti pirite e marcasite ottenuti mediante dragaggio nella Baia di Levante a Vulcano. I campioni sono stati raccolti da J. HONNOREZ.

Element	Concentration range
SiO_2	23.50 - 53.60 wt %
TiO_2	0.30 - 1.55 wt %
Al_2O_3	5.40 - 21.40 wt %
Fe_2O_3	3.66 - 29.30 wt %
MnO	0.01 - 0.13 wt %
MgO	0.01 - 5.28 wt %
CaO	0.28 - 9.36 wt %
Na_2O	0.38 - 3.56 wt %
K_2O	0.62 - 5.20 wt %
P_2O_5	0.13 - 0.82 wt %
LOI	3.80 - 43.30 wt %
S	0.83 - 23.90 wt %
Ag	<0.5 - 4.9 ppm
As	<0.5 - 100 ppm
Au	<2 - 582 ppb
Ba	110 - 920 ppm
Bi	<2 ppm
Cd	<0.5 - 1.0 ppm
Co	6 - 130 ppm
Cu	26 - 350 ppm
Hg	<1 - 12 ppm
Mo	1.3 - 13 ppm
Ni	<1 - 220 ppm
Pb	4 - 62 ppm
Sb	<0.1 - 2.4 ppm
Sr	<10 - 2,300 ppm
V	81 - 770 ppm
Zn	21 - 230 ppm

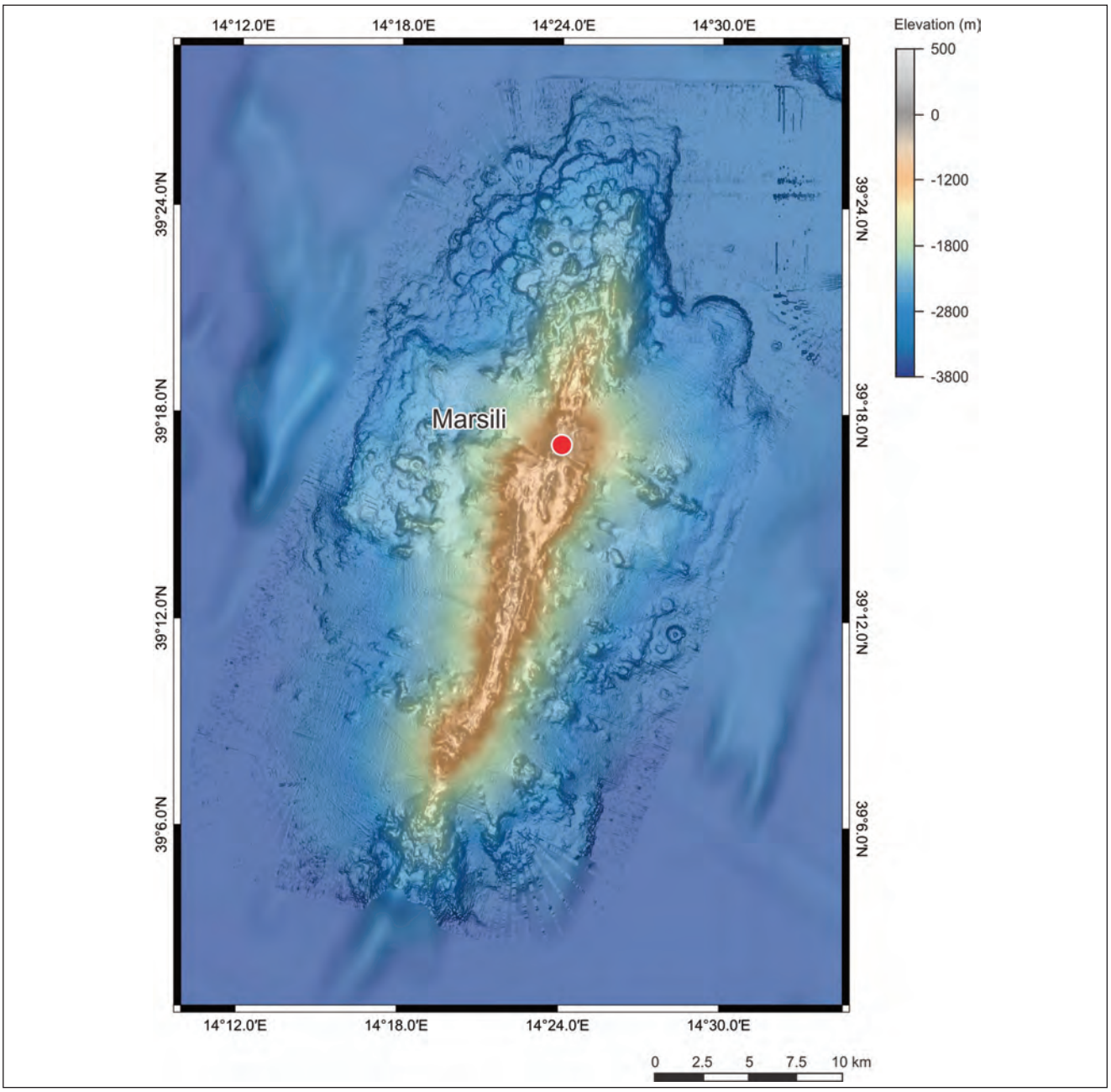

Fig. 13 - Bathymetric map of the Marsili seamount in the southeastern Tyrrhenian Sea. The edifice represents the superinflated spreading ridge of the Marsili back-arc basin. The red circle highlights the location of the low-temperature vent field identified in the summit area of the volcanic edifice. Shipboard bathymetric data was obtained during R/V Meteor cruise M73/2. Gridding was performed using a 30 m grid-cell size. To allow coverage of the entire area shown, the bathymetric data was combined with the global multi-resolution topography data of RYAN *et alii* (2009), which was gridded using a 90 m grid-cell size.
- Mappa batimetrica del seamount Marsili nel Mar Tirreno sud-orientale. L'edificio rappresenta la dorsale di espansione del bacino di retroarco del Marsili. Il cerchio rosso evidenzia la posizione del campo di emissione a bassa temperatura identificato nell'area sommitale dell'edificio vulcanico. I dati batimetrici sono stati ottenuti durante la crociera Meteor R/V, M73/2. La griglia è stata eseguita utilizzando una dimensione della cella di 30 m. Per consentire la copertura dell'intera area mostrata, i dati batimetrici sono stati combinati con quelli globali, multi risoluzione di RYAN et alii (2009), basati su una griglia con dimensione della cella di 90 m.

The occurrence of metalliferous sediments in the summit area of the Marsili seamount at a water depth of ~500 m was first noted in 1986 (DEKOV & SAVELLI, 2004). A sample of yellow-brown ochre having a massive texture was recovered (DEKOV *et alii*, 2006). Seafloor imaging along traverses across the summit region of the volcano onboard R/V Starella in June 1988 revealed the presence of numerous mounds and low-relief chimney structures having an earthy-like texture. A sample recovered from these chimney structures was predominately composed of Fe-Mn-oxide and nontronite. The site was revisited and mapped in August 1988 during a cruise of R/V Knorr (UCHUPI *et alii*, 1988; UCHUPI & BALLARD, 1989). Submersible observations onboard R/V Academic M. Keldysh in August 1988 confirmed the occurrence of hydrothermal activity in the summit region of the volcano where soft, yel-

low and orange colored deposits as well as sites of shimmering water discharge were observed (SAVELLI, 1992; SBORSHCHIKOV & AL'MUKHAMEDOV, 1992). A sample collected during submersible diving at a water depth of ~520 m was found to be compositionally similar to the material recovered in 1986 (DEKOV *et alii*, 2006). Low-temperature hydrothermal discharge in the summit region of Marsili was also observed in 1989 aboard R/V Star Hercules (UCHUPI & BALLARD, 1989). During R/V Urania cruise MAR98 in 1998, a massive sulfide sample with abundant barite was recovered during dredging (station MRS09) in a water depth of ~630 m to the northeast of the summit implying that hydrothermal activity may be more widespread than suggested by the previous observations (MARANI *et alii*, 1999).

A detailed seafloor video survey (station 746ROV) of the summit area of the Marsili seamount was conducted during R/V Poseidon cruise POS340 in 2006 using a remotely operated vehicle (PETERSEN & MONECKE, 2008). The summit area is characterized by massive mafic lava flows flanked by talus breccia. The basalt is covered by variably thick hemipelagic sediment suggesting that the effusive eruptions are not recent. Approaching the low-temperature vent site, widespread orange staining of the hemipelagic sediment could be observed. The vent field itself is approximately 150 m in diameter and located at a water depth of 497-511 m below sea-level. The vent field is characterized by numerous up to 2 m high spires and mounds consisting of Fe-Mn-oxides (fig. 14). The hydrother-

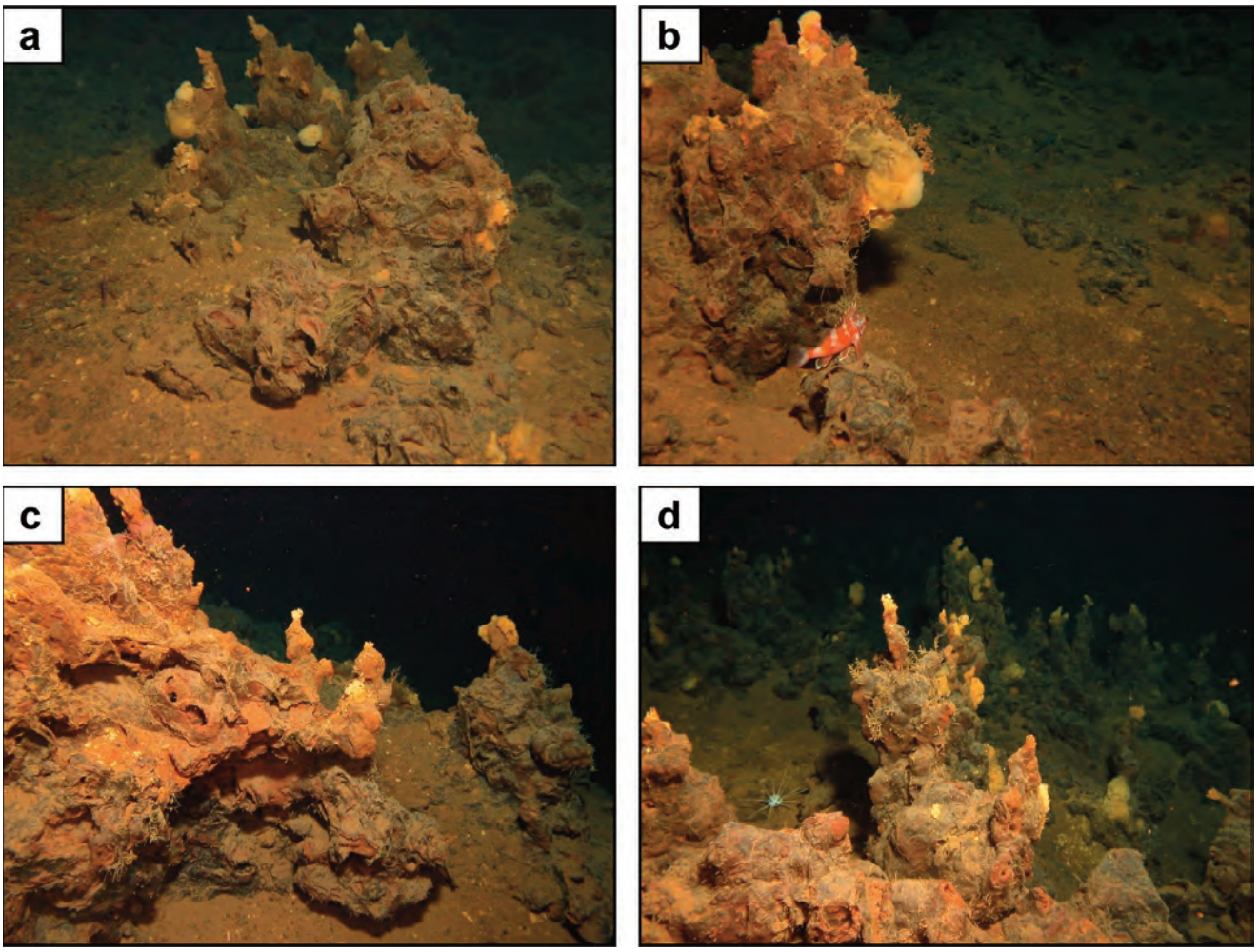

Fig. 14 - Seafloor images of Fe-Mn-oxide chimneys and mounds at the Marsili seamount in the Tyrrhenian Sea. a) Mound composed of Fe-Mn-oxide. The orifices are capped by white to light yellow bacterial matter suggesting that low-temperature fluid flow is ongoing. b) Complex shaped Fe-Mn-oxide mound. c) Mound consisting of hydrothermal precipitates having a laminated appearance. d) Image of the low-temperature vent field showing numerous chimneys and mound-like structures in the background. The vent field is located in the summit area of the Marsili volcanic edifice in a water depth of ~500 m. Field of view is approximately 2 m. Images obtained during station 746ROV of R/V Poseidon cruise POS340 in 2006.
- Immagini di camini e mound di ossidi di Fe-Mn sul fondale marino presso il seamount Marsili, nel Mar Tirreno. a) Mound composto da ossidi di Fe-Mn. I punti di emissione sono ricoperti da una sostanza batterica di colore da bianco a giallo chiaro che suggerisce che sia in corso flusso di fluido a bassa temperatura. b) Mound di forma complessa di ossidi di Fe-Mn. c) Mound costituito da precipitati idrotermali con aspetto laminato. d) Immagine del campo di emissione a bassa temperatura che mostra sullo sfondo numerosi camini e strutture tipo mound. Il campo di emissione si trova nell'area sommitale dell'edificio vulcanico Marsili ad una profondità di ~500 m. Il campo visivo è di circa 2 m. Immagini ottenute durante la calata 746ROV della crociera Poseidon R/V, POS340 nel 2006.

mal deposits are soft and disintegrated easily when touched with the manipulator arm of the remotely operated vehicle. Many of the spires and mounds have orifices capped by white to light yellow bacterial matter (fig. 14), suggesting that low-temperature fluid flow is still occurring. This is cooperated by the observation of shimmering water, indicating discharge of waters having temperatures above ambient. However, no bottom water temperature anomaly was detected (Petersen & Monecke, 2008).

The chimneys at the low-temperature vent site near the summit of Marsili volcano were sampled in 2007 using a TV-guided grab (station 919TVG) during R/V Meteor cruise M73/2 (Petersen & Monecke, 2009). A range of red-brown Fe-Mn-oxide crusts having a laminated appearance or distinct chimney-like shapes were recovered. Geochemical analyses revealed that the samples contain high Fe_2O_3 and MnO contents and are anomalous in As, Ba, Co, Cu, Mo, and V (tab. 4). None of the recovered samples contained sulfide minerals. Drilling of the Fe-Mn-oxide deposits was not successful, presumably due to the soft nature of the hydrothermal precipitates (Petersen & Monecke, 2009).

Seafloor surveying along the crest of Marsili volcano was also conducted during a cruise by R/V Daedalus in May 2011 using a remotely operated vehicle. The field of Fe-Mn-oxide chimneys in the summit area of Marsili was revisited. Similar to the observations of previous expeditions, a large number of individual spires ranging up to 3 m in size were encountered. An additional area with low-temperature hydrothermal precipitates and possible sulfide deposits was discovered to the south of the summit area in a water depth of ~600 m (Ligi *et alii*, 2014). Magnetic field data indicates the presence of a large area of reduced magnetization in this area, which may result from hydrothermal alteration of the basalt (Caratori Tontini *et alii*, 2010, 2014; Caso *et alii*, 2010; Italiano *et alii*, 2014). Water column data indeed suggests that multiple sites of hydrothermal discharge may be present at Marsili (Lupton *et alii*, 2011; Italiano *et alii*, 2014).

7. - DISCUSSION

7.1. - Water depth of sulfide formation

Hydrothermal venting in modern volcanic arcs typically occurs at depths in excess of 1,000 m below sea-level (Monecke *et alii*, 2014). By comparison, the hydrothermal sites of the Aeolian archipelago are located in comparably shallow water because the Aeolian arc rests on buoyant, up to ~20 km thick continental crust (Morelli *et alii*, 1975; Wang *et alii*, 1989; Ventura *et alii*, 1999; Peccerillo *et alii*, 2006).

Tab. 4 - *Ranges of major and trace element concentrations in Fe-Mn-oxide samples (n = 10) recovered from the low-temperature hydrothermal site located close to the summit of the Marsili seamount in ~500 m water depth. The samples were collected during station 919TVG of R/V Meteor cruise M73/2.*

- Intervalli di concentrazione degli elementi maggiori e in traccia in campioni (n = 10) di ossidi di Fe-Mn recuperati dal sito idrotermale a bassa temperatura situato vicino alla sommità del seamount Marsili, a ~500 m profondità. I campioni sono stati raccolti durante la calata 919TVG della crociera Meteor R/V, M73/2.

Element	Concentration range
SiO_2	13.64 - 29.07 wt %
TiO_2	0.01 - 0.11 wt %
Al_2O_3	0.31 - 2.30 wt %
Fe_2O_3	33.63 - 54.16 wt %
MnO	0.48 - 17.37 wt %
MgO	0.82 - 1.02 wt %
CaO	0.57 - 0.88 wt %
Na_2O	1.99 - 3.67 wt %
K_2O	0.48 - 1.03 wt %
P_2O_5	0.57 - 3.05 wt %
LOI	16.80 - 27.40 wt %
S	0.10 - 0.20 wt %
Ag	<0.5 - 1.3 ppm
As	1,040 - 8,130 ppm
Au	<1 - 5 ppb
Ba	116 - 771 ppm
Bi	<2 - 8 ppm
Cd	<0.5 - 2.2 ppm
Co	5.2 - 120 ppm
Cu	<1.0 - 867 ppm
Hg	<1.0 ppm
Mo	61 - 51 ppm
Ni	3.0 - 30 ppm
Pb	9.0 - 29 ppm
Sb	1.1 - 8.8 ppm
Sr	152 - 242 ppm
V	61 - 339 ppm
Zn	9 - 60 ppm

The polymetallic massive sulfate and sulfide mineralization of the Palinuro seamount is located only at a water depth of ~630-650 m below sea-level, making it one of the shallowest massive sulfide deposits currently known. Based on the boiling-point-to-depth curve of seawater (BISCHOFF & ROSENBAUER, 1984), mineralization at the Palinuro seamount may have occurred at maximum temperatures of ~280°C. The high metal grades encountered in drill core demonstrate that metal transport must have been possible in the ore-forming fluids at temperature significantly below those normally observed in deep marine black smokers. This is of particular significance as the solubility of Cu in black smoker fluids decreases with temperature and is negligibly low at temperatures below 300°C (HANNINGTON *et alii*, 1995; GALLANT & VON DAMM, 2006). This may suggest that the mineralizing fluids at Palinuro were of deviating chemical character allowing significant Cu transport towards lower temperatures.

Aside of the massive sulfide mineralization at the Palinuro seamount, venting at comparably shallow water has so far only been encountered in the Tonga and Mariana arcs. In the Tonga arc, two shallow polymetallic sulfide occurrences are located at Volcano 19 (STOFFERS *et alii*, 2006). Focused, high-temperature venting at up to 265°C was observed at a water depth of 540 m from the orifices of several ~2-m-high chimneys that are surrounded by low-relief mounds of barite and anhydrite. The chimneys have thick walls of barite and anhydrite with central conduits filled by fine-grained pyrite, marcasite, sphalerite, and rare chalcopyrite. Additional clusters of up to 7-m-high chimneys occur at a water depth of 420 to 435 m on the central cone complex. A maximum temperature of 253°C was observed at a water depth of 433 m (STOFFERS *et alii*, 2006). In the Mariana arc, polymetallic sulfide mineralization in comparably shallow water occurs at the Black Forest site on the East Diamante volcano. The active vent site is located at a water depth of only 345 m on the flank of a resurgent dome within the large summit caldera. Venting occurs from numerous small mounds and sulfide chimneys that reach a maximum height of 9 m (MERLE *et alii*, 2004). Recovered chimney fragments are composed of varying amounts of barite, silica, and sphalerite, with minor galena, chalcopyrite, and pyrite (HEIN *et alii*, 2014). A maximum vent temperature of 239°C was observed (MERLE *et alii*, 2004).

Although sulfide minerals are only of minor abundance, the massive sulfate deposits located northeast of the Secca dei Panarelli at Panarea in a water depth of ~55-85 m contain polymetallic sulfides (GAMBERI *et alii*, 1997; MARANI *et alii*, 1997; SAVELLI *et alii*, 1999; PETERSEN & MONECKE, 2008; MONECKE *et alii*, 2009; this study). In addition to pyrite and marcasite, minor amounts of sphalerite have been recognized. Core samples contain elevated concentrations of the epithermal-suite of elements Ag, As, Ba, Cd, Hg, Pb, Sb, and Zn, which is consistent with the shallow water conditions at which the mineralization has formed. Based on the boiling-point-to-depth curve of seawater (BISCHOFF & ROSENBAUER, 1984), sulfate and sulfide precipitation could not have occurred at temperatures exceeding 160-180°C. In addition to the vent field northeast of the Secca dei Panarelli, the formation of base metal sulfides and sulfosalts has been observed at the discharge site of up to 137°C hot thermal waters at 23.5 m water depth northwest of Lisca Nera and east of Dattilo (BECKE *et alii*, 2009; VOLTATTORNI *et alii*, 2009; CONTE & CARAMANNA, 2010; this study). This site currently represents the shallowest site of polymetallic sulfide mineralization discovered in the worlds' oceans (MONECKE *et alii*, 2014).

The formation of pyrite and marcasite in the littoral zone of arc volcanoes is not unusual and has been documented at various locations in addition to the Baia di Levante at Vulcano Island. Examples include those in 60 to 110 m water depth at Esmeralda Bank in the Mariana arc (STÜBEN *et alii*, 1992), in 10 to 30 m offshore Kueishantao Island in Taiwan (CHEN *et alii*, 2005; YANG *et alii*, 2005), and in <10 m water depth in the Palaeohori Bay at Milos in the Hellenic arc (VALSAMI-JONES *et alii*, 2005).

7.2. - SUBSEAFLOOR OCCURRENCE OF MASSIVE SULFATE AND SULFIDE DEPOSITS

Research on the hydrothermal occurrences of the Tyrrhenian Sea highlights the importance of host rock controls on the nature of seafloor hydrothermal systems and related mineral deposits. The vent field at the Marsili seamount is hosted by massive lavas. Low-temperature fluid flow presumably occurs along faults and contacts between pillows and massive flows as these represent zones of high permeability. Chimneys and mounds of Fe-Mn oxide are formed at the seafloor as a result of the quenching of the low-temperature hydrothermal fluids and the mixing of the fluids with the cold seawater. Exposures of lava are present throughout the hydrothermal field suggesting that the thickness of the hydrothermal precipitates is only limited.

In contrast to Marsili, mineralization at the Palinuro seamount is entirely buried below a cover of unconsolidated mud containing thin intercalated volcaniclastic units. With the exception of a few tube worm colonies, subtle sediment discoloration, and the occurrence of shimmering water (MONECKE *et*

alii, 2009; THIEL *et alii*, 2012; PETERSEN *et alii*, 2014), the hydrothermal system has no known seafloor expression. Drilling revealed that the sediment cover ranges from tens of centimeters to over 5 m in thickness. Maximum temperatures of 60°C were measured (PETERSEN *et alii*, 2014), suggesting that fluid flow through the unconsolidated sediments covering the mineralized zone is ongoing. Drilling showed that sediments in contact with the massive sulfates and sulfides are indurated and intensely altered. At the top of the mineralized zone, banding of the sulfates and sulfides locally resembles intensely altered and mineralized bedded sediments (PETERSEN *et alii*, 2014).

The polymetallic sulfate and sulfide mineralization at the Palinuro seamount represents the first blind seafloor sulfide occurrence discovered in an arc setting to date (PETERSEN *et alii*, 2014). The textural observation made in drill core and the absence of chimney fragments suggest that the mineralization at Palinuro formed largely, or perhaps even entirely, through subseafloor infiltration and replacement processes. The mineralization at Palinuro does not represent a massive sulfide mound formed through black smoker activity that was buried below younger sediments during and after waning of the hydrothermal activity.

Volcanological studies on ancient massive sulfide deposits highlight the importance of subseafloor infiltration and replacement processes (GIBSON *et alii*, 1999; DOYLE & ALLEN, 2003; FRANKLIN *et alii*, 2005; PIERCEY, 2015). In many ancient massive sulfide deposits, replacement of permeable host strata appears to have been important in the formation of large sulfide deposits as metal precipitation in the subseafloor is more efficient than deposition on the seafloor, which involves substantial loss of metals into the seawater through black smoker activity (FRANKLIN *et alii*, 2005). In ancient massive sulfide deposits, replacement commonly occurs within pumice-rich mass-flow deposits (MORTON *et alii*, 1991; ALLEN, 1994; ALLEN *et alii*, 1996; MONTELIUS *et alii*, 2007) or poorly compacted, coarse-grained volcaniclastic deposits that are commonly glass-rich (KURODA, 1983; HANNINGTON *et alii*, 1999; MONECKE *et alii*, 2008). The depth of replacement below the seafloor is typically difficult to constrain in ancient deposits. However, in the well-studied Rosebery-Hercules deposit in the Cambrian Mount Read volcanic belt of Tasmania (ALLEN, 1994) and at Thalanga in the Ordovician Mound Windsor volcanic belt of Queensland (HILL, 1996), the top of the replacement and infiltration zones was probably also located only within a few meters of the seafloor.

Processes of subseafloor infiltration and deposition were presumably also important in the formation of the shallow marine hydrothermal deposits at Panarea and Vulcano. The massive sulfates at Panarea form extensive subcrops that are covered by unconsolidated sands. Clear textural evidence for replacement of the sand has not been observed in drill core. However, seafloor observations show that the sand covering the massive sulfates is indurated at the sites of intense gas bubbling and thermal water discharge. Pyrite and marcasite formation in the littoral zone of Vulcano Island clearly occurs through subseafloor infiltration. The sulfide minerals form a cement in the highly permeable volcanic sands in the beach area and offshore within the Baia di Levante. Thin section petrography shows that pyrite and marcasite locally replace glassy fragments in the sand, demonstrating that the replacement of volcanic glass can occur even at low temperatures.

The examples of the subseafloor sulfate and sulfide deposits of the Tyrrhenian Sea illustrate the challenges faced during seafloor exploration in arc environments. Current exploration strategies primarily rely on techniques designed to identify plumes from active hydrothermal systems and visual identification of plume sources. In contrast to lava-dominated mid-ocean ridges and back-arcs, host rocks of arc-related hydrothermal systems may include highly permeable strata that facilitate metal deposition in the subseafloor. In these cases, the hydrothermal signal in the overlying water column may be more subtle and the source of plume signals may be difficult to identify during seafloor surveys. If hydrothermal precipitates would not have been recovered during sediment coring at Palinuro and Panarea (MINNITI & BONAVIA, 1984; GAMBERI *et alii*, 1997; MARANI *et alii*, 1997; SAVELLI *et alii*, 1999), the observed seafloor expressions would not have justified shallow drilling using a lander-type drilling device at both sites. This exemplifies the need for the development of geophysical tools to detect buried sulfate and sulfide deposits in arc environments.

7.3. - MAGMATIC VOLATILE CONTRIBUTIONS TO THE HYDROTHERMAL SYSTEMS

The subseafloor replacement-style massive sulfate and sulfide mineralization at the Palinuro seamount is characterized by an unusual sulfide mineralogy (PETERSEN *et alii*, 2014). The occurrence of polymetallic sulfides such as pyrite, tetrahedrite, famatinite, chalcopyrite, sphalerite, and galena during the main stage of the mineralizing event suggests that the hydrothermal fluids were of intermediate-sulfidation state (PETERSEN *et alii*, 2014). However, the formation of the paragenetically later assemblage of covellite, enargite, and galena required an increase in sulfidation state (PETERSEN *et alii*, 2014). The high-

and very high-sulfidation states necessary to form these sulfide minerals can only be attained by hydrothermal fluids containing magmatic SO_2 and H_2S (EINAUDI *et alii*, 2003). A model involving magmatic volatile contributions to the seafloor hydrothermal system at Palinuro is also supported by the sulfur isotopic signature of the sulfide minerals. PETERS *et alii* (2011) and PETERSEN *et alii* (2014) showed that the low sulfur isotopic ratios of pyrite are at least in part a result of magmatic SO_2 disproportionation during fluid evolution.

A possible link between the subseafloor sulfate and sulfide deposit at Palinuro and an actively degassing porphyry intrusion below the seamount was first suggested by MINNITI & BONAVIA (1984), following the initial discovery of massive sulfides on the western sector of the seamount. These authors pointed out that the sulfide mineralogy of the massive sulfides at Palinuro is similar to vein deposits associated with porphyry copper deposits formed in arc environments. PETERSEN *et alii* (2014) also proposed that the conditions of ore formation at Palinuro were generally similar to those encountered in high-sulfidation epithermal deposits forming on land in association with porphyry copper deposits (WHITE & HEDENQUIST, 1995; SILLITOE & HEDENQUIST, 2003).

Magmatic controls on hydrothermal activity can also be demonstrated for the shallow marine vent sites off Panarea Island. Gas venting in the area of the central islets east of the main island has been observed since historic times. However, quiescent degassing is frequently punctuated by violent gas eruptions such as the one observed in November 2002 (CALIRO *et alii*, 2004; CHIODINI *et alii*, 2006; ESPOSITO *et alii*, 2006). The presence of a large number of gas eruption craters on the seafloor, ranging up to 120 m in diameter, suggests that gas eruptions occurred frequently since the last glacial low-stand of the sea-level (ESPOSITO *et alii*, 2006; MONECKE *et alii*, 2012). CALIRO *et alii* (2004), CARACAUSI *et alii* (2005), CHIODINI *et alii* (2006), CAPACCIONI *et alii* (2007) and TASSI *et alii* (2009) hypothesized that these gas eruptions are a result of perturbation of the hydrothermal system caused by a sudden increase in the feeding rate of magmatic volatiles at depth, which may be linked to a magma injection event. Following the 2002 hydrothermal crisis, high concentrations of magmatic SO_2, HCl, and HF were measured in the gas discharges at Panarea confirming the existence of a degassing magma at depth. It is also important to note that venting of dark colored smoke at 23.5 m water depth northwest of Lisca Nera and east of Dattilo was first observed after the November 2002 crisis (ESPOSITO *et alii*, 2006; TASSI *et alii*, 2009; VOLTATTORNI *et alii*, 2009; CONTE & CARAMANNA, 2010), suggesting that polymetallic sulfide formation at this site was triggered by the recent unrest event.

Not unlike the hydrothermal system at Panarea, hydrothermal venting in the Baia di Levante of Vulcano Island can also be related to magmatic degassing processes taking place at depth. Studies of the fluid chemistry suggest that the fumarolic activity in the beach area is most likely related to the interaction of a deep hot fluid of magmatic derivation with shallow surficial fluids (CHIODINI *et alii*, 1995; CAPASSO *et alii*, 1997).

8. - CONCLUSIONS

Over the past decades, exploration in the Tyrrhenian Sea has resulted in the discovery of a diverse range of seafloor hydrothermal occurrences. Hydrothermal activity and related sulfate and sulfide mineralization have been identified at two of the seven Aeolian Islands and one of the submerged arc volcanoes. Low-temperature hydrothermal activity and related Fe-Mn oxide deposits occur at several of the arc volcanoes, but also at the superinflated back-arc spreading center. The nature of the hydrothermal systems of the Aeolian archipelago and the composition of their associated mineral deposits differ in many respects from those of other seafloor hydrothermal systems. Unusual characteristics include the comparable shallow water depths of hydrothermal venting and mineral precipitation, the significance of subseafloor infiltration and replacement processes, the high- and very high-sulfidation states of the sulfide assemblages, and the importance of magmatic volatile contributions to the seafloor hydrothermal systems.

The hydrothermal systems of the Aeolian archipelago represent unique test sites located within the territorial waters of Italy that could be used for the development and deployment of novel seafloor exploration techniques and monitoring systems. In addition, continued research at these sites could play a key role in understanding metal and volatile cycling on arc volcanoes developed on a continental basement and possible links between seafloor hydrothermal systems and the evolution of subduction-related magmas.

Acknowledgements

D. Dettmar prepared the thin sections of the samples from Palinuro and Panarea. X-ray diffraction analyses on the core samples from Panarea were performed by R. Kleeberg. We thank J. HONNOREZ for providing samples from the Baia di

Levante at Vulcano to the Geological Survey of Canada, which formed the basis for subsequent petrographic studies by SP and TM. Guido Giordano is thanked for providing a sample from the shallow marine vent site at Panarea. TM thanks H. Pichler for initial introduction to the hydrothermal sites at Vulcano and Panarea. TM was supported by the Emmy-Noether Program of the German Research Foundation during the initial stages of the research. Funding for the research cruises of R/V Poseidon in 2006 (POS340), 2011 (POS412), and 2012 (POS442) and of R/V Meteor in 2007 (M73/2) and 2012 (M86/4) was provided by the German Science Foundation, the Helmholtz Centre for Ocean Research Kiel, and Neptune Minerals.

REFERENCES

Aliani S., Bortoluzzi G., Caramanna G. & Raffa F. (2010) - *Seawater dynamics and environmental settings after November 2002 gas eruption off Bottaro (Panarea, Aeolian islands, Mediterranean Sea)*. Cont. Shelf Res., **30**: 1338-1348.

Allen R.L. (1994) - *Synvolcanic, subseafloor replacement model for Rosebery and other massive sulfide ores*. Geol. Soc. Australia Abstr., **39**: 89-91.

Allen R.L., Weihed P. & Svenson S.Å. (1996) - *Setting of Zn-Cu-Au-Ag massive sulfide deposits in the evolution and facies architecture of a 1.9 Ga marine volcanic arc, Skellefte district, Sweden*. Econ. Geol., **91**: 1022-1053.

Amend J.P., Rogers K.L., Shock E.L., Gurrieri S. & Inguaggiato S. (2003) - *Energetics of chemolithoautotrophy in the hydrothermal system of Vulcano island, southern Italy*. Geobiol., **1**: 37-58.

Anzidei M., Esposito A., Bortoluzzi G. & De Giosa F. (2005) - *The high resolution bathymetric map of the exhalative area of Panarea (Aeolian islands, Italy)*. Ann. Geophys., **48**: 899-921.

Argnani A. & Savelli C. (1999) - *Cenozoic volcanism and tectonics in the southern Tyrrhenian Sea: Space-time distribution and geodynamic significance*. J. Geodyn., **27**: 409-432.

Bagnato E., Oliveri E., Acquavita A., Covelli S., Petranich E., Barra M., Italiano F., Parello F. & Sprovieri M. (2017) - *Hydrochemical mercury distribution and air-sea exchange over the submarine hydrothermal vents off-shore Panarea island (Aeolian arc, Tyrrhenian Sea)*. Mar. Chem., **194**: 63-78.

Barberi F., Innocenti F., Ferrara G., Keller J. & Villari L. (1974) - *Evolution of Eolian arc volcanism (southern Tyrrhenian Sea)*. Earth Planet. Sci. Lett., **21**: 269-276.

Bargossi G.M., Campos Venuti M., Gasparotto G. & Rossi P.L. (1989) - *Petrologia e stratigrafia delle successioni andesitiche l.s. Di Lipari, Isole Eolie, Italia*. Miner. Petrogr. Acta, **32**: 295-326.

Beccaluva L., Gabbianelli G., Lucchini F., Rossi P.L. & Savelli C. (1985) - *Petrology and K/Ar ages of volcanics dredged from the Eolian seamounts: Implications for geodynamic evolution of the southern Tyrrhenian basin*. Earth Planet. Sci. Lett., **74**: 187-208.

Becke R., Merkel B. & Pohl T. (2009) - *Mineralogical and geochemical characteristics of the shallow-water massive sulfide precipitates of Panarea, Aeolian islands, Italy*. Freiberg Online Geol., **22**: 94-100.

Bergeat A. (1899) - *Die Äolischen Inseln (Stromboli, Panarea, Salina, Lipari, Vulcano, Filicudi, Alicudi)*. Abh. Bayer. Akad. Wiss. München, **20**: 1-274.

Berkenbosch H.A., de Ronde C.E.J., Gemmell J.B., McNeill A.W. & Goemann K. (2012) - *Mineralogy and formation of black smoker chimneys from Brothers submarine volcano, Kermadec arc*. Econ. Geol., **107**: 1613-1633.

Bernauer F. (1933) - *Rezente Erzbildung auf der Insel Vulcano*. Fortschr. Min. Krist. Petr., **17**, 28.

Bernauer F. (1940) - *Rezente Erzbildung auf der Insel Vulcano*. Teil II. Neues Jahrb. Mineral. Beil., **75**: 54-71.

Bialas J. (2015) - *R/V Poseidon cruise report POS484/2 - MARSITE: Seismic investigations at the Palinuro volcanic complex*. GEOMAR Helmholtz-Zentrum für Ozeanforschung Kiel, Germany, 18 pp.

Bigazzi G., Laurenzi M.A., Soligo M. & Tuccimei P. (2008) - *Multi-method approach to dating glass: The case of Basiluzzo islet (Aeolian archipelago, Italy)*. J. Volcanol. Geotherm. Res., **177**: 244-250.

Bischoff J.L. & Rosenbauer R.J. (1984) - *The critical point and two-phase boundary of seawater, 200-500°C*. Earth Planet. Sci. Lett., **68**: 172-180.

Boatta F., D'Alessandro W., Gagliano A.L., Liotta M., Milazzo M., Rodolfo-Metalpa R., Hall-Spencer J.M. & Parello F. (2013) - *Geochemical survey of Levante Bay, Vulcano island (Italy), a natural laboratory for the study of ocean acidification*. Mar. Pollut. Bull., **73**: 485-494.

Boccaletti M., Nicholich R. & Tortorici L. (1984) - *The Calabrian arc and the Ionian Sea in the dynamic evolution of the central Mediterranean*. Mar. Geol., **55**: 219-245.

Bonatti E., Honnorez J., Joensuu O. & Rydell H. (1972) - *Submarine iron deposits from the Mediterranean Sea*. In: Stanley D.J. (Ed.), The Mediterranean Sea: *A Natural Sedimentation Laboratory*. Dowden, Hutchinson & Ross, Stroudsburg, Pennsylvania, 701-710.

Bosman A., Chiocci F.L. & Romagnoli C. (2009) - *Morpho-structural setting of Stromboli volcano revealed by high-resolution bathymetry and backscatter data of its submarine portions*. Bull. Volcanol., **71**: 1007-1019.

Breuer C. (2010) - *The role of magmatic volatiles within the formation of sulfates and sulfides in the off-shore area of Panarea, Aeolian island arc, Italy*. Unpublished M.Sc. Thesis, Westfälische Wilhelms-Universität Münster, Germany, 105 pp.

Brusilovskiy Y.V. & Gorodnitskiy A.M. (1990) - *Evolution of basaltic volcanic activity and development of seamounts in the Tyrrhenian basin as indicated by geomagnetic data*. Geotectonics, **24**: 350-358.

Calanchi N., Capaccioni B., Martini M., Tassi F. & Valentini L. (1995) - *Submarine gas-emission from Panarea island (Aeolian archipelago): Distribution of inorganic and organic compounds and inferences about source conditions*. Acta Vulcan., **7**: 43-48.

Calanchi N., Tranne C.A., Lucchini F., Rossi P.L. & Villa I.M. (1999) - *Explanatory notes to the geological map (1:10,000) of Panarea and Basiluzzo islands (Aeolian arc, Italy)*. Acta Vulcan., **11**: 223-243.

Caliro S., Caracausi A., Chiodini G., Ditta M., Italiano F., Longo M., Minopoli C., Nuccio P.M., Paonita A. & Rizzo A. (2004) - *Evidence of a recent input of magmatic gases into the quiescent volcanic edifice of Panarea, Aeolian islands, Italy*. Geophys. Res. Lett., **31**: L07619, doi: 10.1029/2003GL019359.

Capaccioni B., Tassi F. & Vaselli O. (2001) - *Organic and inorganic geochemistry of low temperature gas discharges at the Baia di Levante beach, Vulcano island, Italy. J*. Volcanol. Geotherm. Res., **108**: 173-185.

Capaccioni B., Tassi F., Vaselli O., Tedesco D. & Poreda R. (2007) - *Submarine gas burst at Panarea island (southern Italy) on 3 November 2002: A magmatic versus hydrothermal episode*. J. Geophys. Res., **112**: B05201, doi: 10.1029/2006JB004359.

Capasso G., Favara R., Francofonte S. & Inguaggiato S. (1999) - *Chemical and isotopic variations in fumarolic discharges and thermal waters at Vulcano island (Aeolian islands, Italy) during 1996: Evidence of resumed volcanic activity*. J. Volcanol. Geotherm. Res., **88**: 167-175.

Capasso G., Favara R. & Inguaggiato S. (1997) - *Chemical features and isotopic composition of gaseous manifestations on Vulcano island, Aeolian islands, Italy: An interpretative model of fluid circulation*. Geochem. Cosmochim. Acta, **61**: 3425-3440.

Caracausi A., Ditta M., Italiano F., Longo M., Nuccio P.M., Paonita A. & Rizzo A. (2005) - *Changes in fluid geochemistry and physico-chemical conditions of geothermal systems caused by magmatic input: The recent abrupt outgassing off the island of Panarea (Aeolian islands, Italy)*. Geochim. Cosmochim. Acta, **69**: 3045-3059.

Caramanna G., Espa S. & Bouchè V. (2010) - *Study of the environmental effects of submarine CO_2-rich emissions by means of scientific diving techniques (Panarea island - Italy)*. Int. J. Soc. Under. Tech., **29**: 79-85.

Caratori Tontini F., Bortoluzzi G., Carmisciano C., Cocchi L., de Ronde C.E.J., Ligi M. & Muccini F. (2014) - *Near-bottom magnetic signatures of submarine hydrothermal systems at Marsili and Palinuro volcanoes, southern Tyrrhenian Sea, Italy*. Econ. Geol., **109**: 2119-2128.

Caratori Tontini F., Cocchi L., Muccini F., Carmisciano C., Marani M., Bonatti E., Ligi M. & Boschi E. (2010) - *Potential-field modeling of collapse-prone submarine volcanoes in the southern Tyrrhenian Sea (Italy)*. Geophys. Res. Lett., **37**, L03305, doi: 10.1029/2009GL041757.

Caso C., Signanini P., de Santis A., Favali P., Iezzi G., Marani M.P., Paltrinieri D., Rainone M.L. & Di Sabatino B. (2010) - *Submarine geothermal systems in southern Tyrrhenian Sea as future energy resource: The example of Marsili seamount*. Proceedings Word Geothermal Congress 2010, Bali, Indonesia, 25-29 April 2010, 7 pp.

Castellarin A. & Sartori R. (1978) - *Quaternary iron-manganese deposits and associated pelagic sediments (radiolarian clay and chert, gypsiferous mud) from the Tyrrhenian Sea*. Sedimentology, **25**: 801-821.

Chen C.T.A., Zeng Z., Kuo F.W., Yang T.F., Wang B.J. & Tu Y.Y. (2005) - *Tide-influenced acidic hydrothermal system offshore NE Taiwan*. Chem. Geol., **224**: 69-81.

Chiarabba C., Pino N.A., Ventura G. & Vilardo G. (2004) - *Structural features of the shallow plumbing system of Vulcano island, Italy*. B. Volcanol., **66**: 477-484.

Chiodini G., Caliro S., Caramanna G., Granieri D., Minopoli C., Moretti R., Perotta L. & Ventura G. (2006) - *Geochemistry of the submarine gaseous emissions of Panarea (Aeolian islands, southern Italy): Magmatic vs. Hydrothermal origin and implications for volcanic surveillance*. Pure Appl. Geophys., **163**: 759-780.

Chiodini G., Cioni R. & Marini L. (1993) - *Reactions governing the chemistry of crater fumaroles from Vulcano island, Italy, and implications for volcanic surveillance*. Appl. Geochem., **8**: 357-371.

Chiodini G., Cioni R., Marini L. & Panichi C. (1995) - *Origin of the fumarolic fluids of Vulcano island, Italy and implications for volcanic surveillance*. B. Volcanol., **57**: 99-110.

Cioni R. & D'Amore F. (1984) - *A genetic model for the crater fumaroles of Vulcano island (Sicily, Italy)*. Geothermics, **13**: 375-384.

Clocchiatti R., Del Moro A., Gioncada A., Joron J.L., Mosbah M., Pinarelli L. & Sbrana A. (1994) - *Assessment of a shallow magmatic system: The 1888-90 eruption, Vulcano island, Italy*. Bull. Volcanol., **56**: 466-486.

Colantoni P., Lucchini F., Rossi P.L., Sartori R. & Savelli C. (1981) - *The Palinuro volcano and magmatism of the southeastern Tyrrhenian Sea (Mediterranean)*. Mar. Geol., **39**: 1-12.

Conte A.M. & Caramanna G. (2010) - *Preliminary characterisation of a shallow water hydrothermal sulphide deposit recovered by scientific divers (Aeolian islands, southern Tyrrhenian Sea)*. Int. J. Soc. Under. Tech., **29**: 109-115.

Cortese M., Frazzetta G. & La Volpe L. (1986) - *Volcanic history of Lipari (Aeolian islands, Italy) during the last 10,000 years*. J. Volcanol. Geotherm. Res., **27**: 117-133.

De Astis G., Lucchi F., Dellino P., La Volpe L., Tranne C.A., Frezzotti M.L. & Peccerillo A. (2013) - *Geology, volcanic history and petrology of Vulcano (central Aeolian archipelago)*. Geol. Soc. Lond. Mem., **37**: 281-349.

de Ronde C.E.J., Hannington M.D., Stoffers P., Wright I.C., Ditchburn R.G., Reyes A.G., Baker E.T., Massoth G.J., Lupton J.E., Walker S.L., Greene R.R., Soong C.W.R., Ishibashi J., Lebon G.T., Bray C.J. & Resing J.A. (2005) - *Evolution of a submarine magmatic-hydrothermal system: Brothers volcano, southern Kermadec arc, New Zealand*. Econ. Geol., **100**: 1097-1133.

de Ronde C.E.J., Massoth G.J., Baker E.T. & Lupton J.E. (2003) - *Submarine hydrothermal venting related to volcanic arcs*. SEG Spec. Pub., **10**: 91-110.

de Ronde C.E.J., MassoTH G.J., Butterfield D.A., Christenson B.W., Ishibahi J., Ditchburn R.G., Hannington M.D., Brathwaite R.L., Lupton J.E., Kamenetsky V.S., Graham I.J., Zellmer G.F., Dziak R.P., Embley R.W., Dekov V.M., Munnik F., Lahr J., Evans L.J. & Takai K. (2011) - *Submarine hydrothermal activity and gold-rich mineralization at Brothers Volcano, Kermadec arc, New Zealand. Miner*. Dep., **46**: 541-584.

de Ronde C.E.J., Walker S.L., Ditchburn R.G., Caratori Tontini F., Hannington M.D., Merle S.G., Timm C., Handler M.R., Wysoczanski R.J., Dekov V.M., Kamenov G.D., Baker E.T., Embley R.W., Lupton J.E. & Stoffers P. (2014) - *The anatomy of a buried submarine hydrothermal system, Clark volcano, Kermadec arc, New Zealand*. Econ. Geol., **109**: 2261-2292.

Dekov V.M., Kamenov G.D., Savelli C. & Stummeyer J. (2006) - *Anthropogenic Pb component in hydrothermal ochres from Marsili seamount (Tyrrhenian Sea)*. Mar. Geol., **229**: 199-208.

Dekov V.M. & Savelli C. (2004) - *Hydrothermal activity in the SE Tyrrhenian Sea: An overview of 30 years of research*. Mar. Geol., **204**: 161-185.

Del Monte M. (1972) - *Il vulcanesimo del Mar Tirreno: Nota preliminare sui vulcani Marsili e Palinuro*. G. Geol., **38**: 231-252.

Del Moro A., Gioncada A., Pinarelli L., Sbrana A. & Joron J.L. (1998) - *Sr, Nd, and Pb isotope evidence for open system evolution at Vulcano, Aeolian arc, Italy*. Lithos, **43**: 81-106.

Dellino P. & La Volpe L. (1995) - *Fragmentation versus transportation mechanisms in the pyroclastic sequence of Monte Pilato - Rocche Rosse (Lipari, Italy)*. J. Volcanol. Geotherm. Res., **64**: 211-231.

Diliberto I.S. (2017) - *Long-term monitoring on a closed-conduit volcano: A 25 year long time-series of temperatures recorded at La Fossa cone (Vulcano island, Italy), ranging from 250°C to 520°C*. J. Volcanol. Geotherm. Res., **346**: 151-160.

Dolfi D., De Rita D., Cimarelli C., Mollo S., Soligo M. & Fabbri M. (2007) - *Dome growth rates, eruption frequency and assessment of volcanic hazard: Insights from new U/Th dating of the Panarea and Basiluzzo dome lavas and pyroclastics, Aeolian islands, Italy*. Quat. Int., 162-163, 182-194.

Doyle M.G. & Allen R.L. (2003) - *Subsea-floor replacement in volcanic-hosted massive sulfide deposits*. Ore Geol. Rev., **23**: 183-222.

Eckhardt J.D., Glasby G.P., Puchelt H. & Berner Z. (1997) - *Hydrothermal manganese crusts from Enarete and Palinuro seamounts in the Tyrrhenian Sea*. Mar. Georesour. Geotec., **15**: 175-208.

Einaudi M.T., Hedenquist J.W. & Inan E.E. (2003) - *Sulfidation state of fluids in active and extinct hydrothermal systems: Transitions from porphyry to epithermal environments*. SEG Spec. Pub., **10**: 285-313.

Ellam R.M., Hawkesworth C.J., Menzies M.A. & Rogers N.W. (1989) - *The volcanism of southern Italy: Role of subduction and the relationship between potassic and sodic alkaline magmatism*. J. Geophys. Res., **94**: 4589-4601.

Embley R.W., Baker E.T., Butterfield D.A., Chadwick W.W. Jr., Lupton J.E., Resing J.A., De Ronde C.E.J., Nakamura K., Tunnicliffe V., Dower J.F. & Merle S.G. (2007) - *Exploring the submarine ring of fire: Mariana arc-Western Pacific*. Oceanography, **20**: 68-79.

Esposito A., Giordano G. & Anzidei M. (2006) - *The 2002-2003 submarine gas eruption at Panarea volcano (Aeolian islands, Italy): Volcanology of the seafloor and implications for the hazard scenario*. Mar. Geol., **227**: 119-134.

Esposito V., Andaloro F., Canese S., Bortoluzzi G., Bo M., Di Bella M., Italiano F., Sabatino G., Battaglia P., Consoli P., Giordano P., Spagnoli F., La Cono V., Yakimov M.M., Scotti G. & Romeo T. (2018) - *Exceptional discovery of a shallow-water hydrothermal site in the SW area of Basiluzzo islet (Aeolian archipelago, South Tyrrhenian Sea): An environment to preserve*. Plos ONE, **13**, e0190710.

Fabbri A., Marabini F. & Rossi S. (1973) - *Lineamenti geomorphologici del Monte Palinuro e del Monte delle Baronie*. G. Geol., **39**: 133-156.

Fabris M., Baldi P., Anzidei M., Pesci A., Bortoluzzi G. & Aliani S. (2010) - *High resolution topographic model of Panarea island by fusion of photogrammetric, Lidar and bathymetric digital terrain models*. Photogramm. Rec., **25**: 382-401.

Faggion O., Pinna E., Savelli C. & Schreider A.A. (1995) - *Geomagnetism and age study of Tyrrhenian seamounts*. Geophys. J. Int., **123**: 915-930.

Favalli M., Karátson D., Mazzuoli R., Pareschi M.T. & Ventura G. (2005) - *Volcanic geomorphology and tectonics of the Aeolian archipelago (southern Italy) based on integrated DEM data*. B. Volcanol., **68**: 157-170.

Forni F., Lucchi F., Peccerillo A., Tranne C.A., Rossi P.L. & Frezzotti M.L. (2013) - *Stratigraphy and geological evolution of the Lipari volcanic complex (central Aeolian archipelago)*. Geol. Soc. Lond. Mem., **37**: 213-279.

Francalanci L., Lucchi F., Keller J., De Astis G. & Tranne C.A. (2013) - *Eruptive, volcano-tectonic and magmatic history of the Stromboli volcano (north-eastern Aeolian archipelago)*. Geol. Soc. Lond. Mem., **37**: 397-471.

Franklin J.M., Gibson H.L., Jonasson I.R. & Galley A.G. (2005) - *Volcanogenic massive sulfide deposits*. In: Hedenquist J.W., Thompson J.F.H., Goldfarb R.J. & Richards J.P. (Eds), Economic Geology 100th Anniversary Volume. Society of Economic Geologists, Littleton, 523-560.

Fulignati P., Gioncada A. & Sbrana A. (1996) - *Hydrothermal alteration in the subsoil of Porto di Levante, Vulcano (Aeolian islands, Italy)*. Acta Vulcan., **8**: 129-138.

Gabbianelli G., Gillot P.Y., Lanzafame G., Romagnoli C. & Rossi P.L. (1990) - *Tectonic and volcanic evolution of Panarea (Aeolian islands, Italy)*. Mar. Geol., **92**: 313-326.

Gabbianelli G., Romagnoli C., Rossi P.L. & Calanchi N. (1993) - *Marine geology of the Panarea-Stromboli area (Aeolian archipelago, southeastern Tyrrhenian Sea)*. Acta Vulcanol., **3**: 11-20.

Gallant R.M. & Von Damm K.L. (2006) - *Geochemical controls on hydrothermal fluids from the Kairei and Edmond vent fields, 23°-25°S, Central Indian Ridge*. Geochem. Geophys. Geosys., **7**, Q06018, doi: 10.1029/2005GC001067.

Gamberi F. & Marani M.P. (1997) - *Detailed bathymetric mapping of the eastern offshore slope of Lipari island (Tyrrhenian Sea): Insight into the dark side of an arc volcano*. Mar. Geophys. Res., **19**: 363-377.

Gamberi F., Marani M.P. & Savelli C. (1997) - *Tectonic, volcanic and hydrothermal features of a submarine portion of the Aeolian arc (Tyrrhenian Sea)*. Mar. Geol., **140**: 167-181.

Garavelli A., Grasso M.F. & Vurro F. (1996) - *Mineral occurrence and depositional processes at Baia di Levante area (Vulcano island, Italy)*. Mineral. Petrogr. Acta, **39**: 251-261.

Gasparini C., Iannaccone G., Scandone P. & Scarpa R. (1982) - *Seismotectonics of the Calabrian arc*. Tectonophysics, **84**: 267-286.

Ghisetti F. & Vezzani L. (1981) - *Contribution of structural analysis to understanding the geodynamic evolution of the Calabrian arc (southern Italy)*. J. Struct. Geol., **3**: 371-381.

Gibson H.L., Morton R.L. & Hudak G.J. (1999) - *Submarine volcanic processes, deposits, and environments favorable for the location of volcanic-associated massive sulfide deposits*. Rev. Econ. Geol., **8**: 13-51.

Gillot P.Y. (1987) - *Histoire volcanique des Iles Eoliennes: Arc insulaire ou complexe orogénique anulaire?* Doc. Trav. Inst. Géol. Albert-de-Lapparent Paris, **11**: 35-42.

Gugliandolo C., Italiano F. & Maugeri T.L. (2006) - *The submarine hydrothermal system of Panarea (southern Italy): Biogeochemical processes at the thermal fluids-sea bottom interface*. Ann. Geophys., **49**: 783-792.

Gugliandolo C., Lentini V., Bunk B., Overmann J., Italiano F. & Maugeri T.L. (2015) - *Changes in prokaryotic community composition accompanying a pronounced temperature shift of a shallow marine thermal brine pool (Panarea island, Italy)*. Extremophiles, **19**: 547-559.

Gugliandolo C., Lentini V., Spanò A. & Maugeri T.L. (2012) - *New bacilli from shallow hydrothermal vents of Panarea island (Italy) and their biotechnological potential*. J. Appl. Microbiol., **112**: 1102-1112.

Hannington M.D., Bleeker W. & Kjarsgaard I. (1999) - *Sulfide mineralogy, geochemistry, and ore genesis of the Kidd Creek deposit: Part I. North, Central, and South orebodies*. Econ. Geol. Monogr., **10**: 163-224.

Hannington M.D., de Ronde C.E.J. & Petersen S. (2005) - *Sea-floor tectonics and submarine hydrothermal systems*. In: Hedenquist J.W., Thompson J.F.H., Goldfarb R.J. & Richards J.P. (Eds), Economic Geology 100th Anniversary Volume. Society of Economic Geologists, Littleton, 111-141.

Hannington M.D., Jonasson I.R., Herzig P.M. & Petersen S. (1995) - *Physical and chemical processes of seafloor mineralization at mid-ocean ridges*. Geophys. Monogr. Ser., **91**: 115-157.

Hein J.R., de Ronde C.E.J., Koski R.A., Ditchburn R.G., Mizell K., Tamura Y., Stern R.J., Conrad T.A., Ishizuka O. & Leybourne M.I. (2014) - *Layered hydrothermal barite-sulfide mound field, East Diamante Caldera, Mariana volcanic arc*. Econ. Geol., **100**: 2179-2206.

Heinicke J., Italiano F., Maugeri R., Merkel B., Pohl T., Schipek M. & Braun T. (2009) - *Evidence of tectonic control on active arc volcanism: The Panarea Stromboli tectonic link inferred by submarine hydrothermal vents monitoring (Aeolian arc, Italy)*. Geophys. Res. Lett., **36**, L04301, doi: 10.1029/2008GL036664.

Hill A.P. (1996) - *Structure, volcanic setting, hydrothermal alteration and genesis of the Thalanga massive sulphide deposit*. Unpublished Ph.D. Thesis, University of Tasmania, Hobart, Australia, 404 pp.

Hölz S. (2017) - *R/V Poseidon cruise report POS509 - ELECTROPAL2: Geophysical investigations of sediment hosted massive sulfide deposits on the Palinuro vol-*

canic complex in the Tyrrhenian Sea. Berichte aus dem GEOMAR Helmholtz-Zentrum für Ozeanforschung Kiel, Germany, **39**, 63 pp.

Honnorez J. (1969) - *La formation actuelle d'un gisement sous-marin de sulfures fumerolliens a Vulcano (mer tyrrhénienne). Partie I. Les minéraux sulfurés des tufs immergés à faible profondeur. Miner.* Deposita, **4**: 114-131.

Honnorez J., Honnorez-Guerstein B., Valette J. & Wauschkuhn A. (1973) - *Present day formation of an exhalative sulfide deposit at Vulcano (Tyrrhenian Sea), Part II: Active crystallization of fumarolic sulfides in the volcanic sediments of the Baia di Levante*. In: Amstutz G.C. & Bernard A.J. (Eds), Ores in Sediments. Springer, Berlin, Germany, 139-166.

Honnorez J. & Keller J. (1968) - *Xenolithe in vulkanischen Gesteinen der Äolischen Inseln (Sizilien)*. Geol. Rundsch., **57**: 719-736.

Iezzi G., Caso C., Ventura G., Vallefuoco M., Cavallo A., Behrens H., Mollo S., Paltrinieri D., Signanini P. & Vetere F. (2014) - *First documented deep submarine explosive eruptions at the Marsili seamount (Tyrrhenian Sea, Italy): A case of historical volcanism in the Mediterranean Sea*. Gondwana Res., **25**: 764-774.

Inguaggiato S., Mazot A., Diliberto I.S., Inguaggiato C., Madonia P., Rouwet D. & Vita F. (2012) - *Total CO_2 output from Vulcano island (Aeolian islands, Italy)*. Geochem. Geophys. Geosys., **13**, Q02012, doi: 10.1029/2011GC003920.

Italiano F., de Santis A., Favali P., Rainone M.L., Rusi S. & Signanini P. (2014) - *The Marsili volcanic seamount (southern Tyrrhenian Sea): A potential offshore geothermal resource*. Energies, **7**: 4068-4086.

Italiano F. & Nuccio P.M. (1991) - *Geochemical investigations of submarine volcanic exhalations to the east of Panarea, Aeolian islands, Italy*. J. Volcanol. Geotherm. Res., **46**: 125-141.

Jegen M. (2015) - *R/V Poseidon cruise report POS483 - EMPAL: Electromagnetic investigation of sedimented massive sulphide deposits on the Palinuro volcanic complex in the Tyrrhenian Sea*. Helmholtz-Zentrum für Ozeanforschung Kiel, Germany, 52 pp.

Keller J. (1980) -*The island of Salina*. Rend. Soc. Ital. Mineral. Petrol., **36**: 489-524.

Kidd R.B. & Ármannson H. (1979) - *Manganese and iron micronodules from a volcanic seamount in the Tyrrhenian Sea*. J. Geol. Soc. Lond., **136**: 71-76.

Kokelaar P. & Romagnoli C. (1995) - *Sector collapse, sedimentation and clast-population evolution at an active island-arc volcano: Stromboli, Italy*. Bull. Volcanol., **57**: 240-262.

Kuroda H. (1983) - *Geologic characteristics and formation environments of the Furutobe and Matsuki Kuroko deposits, Akita Prefecture, northeast Japan*. Econ. Geol. Monogr. **5**: 149-166.

Laschek D. (1986) - *Cruise report of R/V Sonne cruise SO41 - HYMAS I: Hydrothermal Massive sulfides*. Universität Karlsruhe, Germany, 331 pp.

Lentini V., Gugliandolo C., Bunk B., Overmann J. & Maugeri T.L. (2014) - *Diversity of prokaryotic community at a shallow marine hydrothermal site elucidated by Illumina sequencing technology*. Curr. Microbiol., **69**: 457-466.

Leybourne M.I., de Ronde C.E.J., Wysoczanski R.J., Walker S.L., Timm C., Gibson H.L., Layton-Matthews D., Baker E.T., Clark M.R., Caratori Tontini F., Faure K., Lupton J.E., Fornari D.J., Soule S.A. & Massoth, G.J. (2012a) - *Geology, hydrothermal activity, and sea-floor massive sulfide mineralization at the Rumble II West mafic caldera*. Econ. Geol., **107**: 1649-1668.

Leybourne M.I., Schwarz-Schampera U., de Ronde C.E.J., Baker E.T., Faure K., Walker S.L., Butterfield D.A., Resing J.A., Lupton J.E., Hannington M.D., Gibson H.L., Massoth G.J., Embley R.W., Chadwick W.W. Jr., Clark M.R., Timm C., Graham I.J. & Wright I.C. (2012b) - *Submarine magmatic-hydrothermal systems at the Monowai volcanic center, Kermadec arc*. Econ. Geol., **107**: 1669-1694.

Ligi M., Cocchi L., Bortoluzzi G., D'Oriano F., Muccini F., Caratori Tontini F., de Ronde C.E.J. & Carmisciano C. (2014) - *Mapping of seafloor hydrothermally altered rocks using geophysical methods: Marsili and Palinuro seamounts, southern Tyrrhenian Sea*. Econ. Geol., **109**: 2103-2117.

Linke P. (2014) -*R/V Poseidon cruise report POS469 - PANAREA: Panarea shallow-water diving campaign*. Report of the Leibniz-Institute of Marine Sciences at the Christian Albrechts University Kiel, Germany, **19**, 50 pp.

Lucchi F., Gertisser R., Keller J., Forni F., De Astis G. & Tranne C.A. (2013c) - *Eruptive history and magmatic evolution of the island of Salina (central Aeolian archipelago)*. Geol. Soc. Lond. Mem., **37**: 155-211.

Lucchi F., Peccerillo A., Tranne C.A., Rossi P.L., Frezzotti M.L. & Donati C. (2013a) - *Volcanism, calderas and magmas of the Alicudi composite volcano (western Aeolian archipelago)*. Geol. Soc. Lond. Mem., **37**: 83-111.

Lucchi F., Santo A.P., Tranne C.A., Peccerillo A. & Keller J. (2013b) -*Volcanism, magmatism, volcano-tectonics and sea-level fluctuations in the geological history of Filicudi (western Aeolian archipelago)*. Geol. Soc. Lond. Mem., **37**: 113-153.

Lucchi F., Tranne C.A., Peccerillo A., Keller J. & Rossi P.L. (2013d) - *Geological history of the Panarea volcanic group (eastern Aeolian archipelago)*. Geol. Soc. Lond. Mem., **37**: 351-395.

Lupton J., Butterfield D., Lilley M., Evans L., Nakamura K., Chadwick W. Jr., Resing J.,

Embley R., Olson E., Proskurowski G., Baker E., de Ronde C., Roe K., Greene R., Lebon G. & Young C. (2006) - *Submarine venting of liquid carbon dioxide on a Mariana arc volcano. Geochem*. Geophys. Geosys., **7**, Q08007, doi:10.1029/2005GC001152.

Lupton J., de Ronde C., Sprovieri M., Baker E.T., Bruno P.P., Italiano F., Walker S., Faure K., Leybourne M., Britten K. & Greene R. (2011) - *Active hydrothermal discharge on the submarine Aeolian arc*. J. Geophys. Res., **116**, B02102, doi: 10.1029/2010JB007738.

Lupton J., Lilley M., Butterfield D., Evans L., Embley R., Massoth G., Christenson B., Nakamura K. & Schmidt M. (2008) - *Venting of a separate CO_2-rich gas phase from submarine arc volcanoes: Examples from the Mariana and Tonga-Kermadec arcs*. J. Geophys. Res., **113**, B08S12, doi: 10.1029/2007JB005467.

Marani M.P., Gamberi F., Casoni L., Carrara G., Landuzzi V., Musacchio M., Penitenti D., Rossi L. & Trua T. (1999) - *New rock and hydrothermal samples from the southern Tyrrhenian Sea: The MAR-98 research cruise*. G. Geol., **61**: 3-24.

Marani M.P., Gamberi F. & Savelli C. (1997) - *Shallow-water polymetallic sulfide deposits in the Aeolian island arc*. Geology, **25**: 815-818.

Marani M.P. & Trua T. (2002) - *Thermal constriction and slab tearing at the origin of a superinflated spreading ridge: Marsili volcano (Tyrrhenian Sea)*. J. Geophys. Res., **107**, 2188, doi: 10.1029/2001JB000285.

Maugeri T.L., Lentini V., Gugliandolo C., Italiano F., Cousin S. & Stackebrandt E. (2009) -*Bacterial and archaeal populations at two shallow hydrothermal vents off Panarea island (Eolian islands, Italy)*. Extremophiles, **13**: 199-212.

Mazzuoli R., Tortorici L. & Ventura G. (1995) - *Oblique rifting in Salina, Lipari and Vulcano islands (Aeolian islands, southern Italy)*. Terra Nova, **7**: 444-452.

McGinnis D.F., Beaubien S.E., Bigalke N., Bryant L.D., Celussi M., Comici C., De Vittor C., Feldens P., Giani M., Karuza A. & Schneider v. Deimling J. (2011) - *Eurofleet's cruise report R/V Urania U10/2011 - paco2: The Panarea natural CO_2 seeps - fate and impact of the leaking gas*. Leibniz-Institute of Marine Sciences at the Christian Albrechts University Kiel, Germany, 55 pp.

Mercalli G. (1883) - *Vulcani e fenomeni vulcanici in Italia*. In: Negri G., Stoppani A., Mercalli G. (Eds), Geologia d'Italia, A. Forni, Milano, 374 pp.

Mercalli G. & Silvestri O. (1891) - *Le eruzioni dell'isola di Vulcano, incominciate il 3 Agosto 1888 e terminate il 22 Marzo 1890*. Ann. Ufficio Centr. Meteorol. Geodin., **10**: 1-213.

Merle S., Ristau S., Embley R.W. & Chadwick W. (2004) - *Cruise report R/V Thomas G. Thompson TN167: Submarine Ring of Fire 2004 - Mariana arc submarine volcanoes*. Pacific Marine Environmental Laboratory, National Oceanic and Atmospheric Administration, Seattle, 274 pp.

Minniti M. & Bonavia F.F. (1984) - *Copper-ore grade hydrothermal mineralization discovered in a seamount in the Tyrrhenian Sea (Mediterranean): Is the mineralization related to porphyry-coppers or to base metal lodes?* Mar. Geol., **59**: 271-282.

Minniti M., Bonavia F.F., Dacquino C. & Raspa G. (1986) - *Distribution of Mn, Fe, Ni, Co, and Cu in young sediments on the Palinuro seamount in the southeast Tyrrhenian Sea (Mediterranean)*. Mar. Mining, **5**: 277-305.

Monecke T., Gibson H., Dubé B., Laurin J., Hannington M.D. & Martin L. (2008) - *Geology and volcanic setting of the Horne deposit, Rouyn-Noranda, Quebec: Initial results of a new research project*. Geol. Surv. Canada Curr. Res., 2008-9, 16 pp.

Monecke T., Köhler S., Kleeberg R., Herzig P.M. & Gemmell J.B. (2001) - *Quantitative phase-analysis by the Rietveld method using X-ray powder-diffraction data: Application to the study of alteration halos associated with volcanic-rock-hosted massive sulfide deposits*. Can. Mineral., **39**: 1617-1633.

Monecke T., Petersen S. & Hannington M.D. (2014) - *Constraints on water depth of massive sulfide formation: Evidence from modern seafloor hydrothermal systems in arc-related settings*. Econ. Geol., **109**: 2079-2101.

Monecke T., Petersen S., Hannington M.D., Anzidei M., Esposito A., Giordano G., Garbe-Schönberg D., Augustin N., Melchert B. & Hocking M. (2012) - *Explosion craters associated with shallow submarine gas venting off Panarea island, Italy*. B. Volcanol., **74**: 1937-1944.

Monecke T., Petersen S., Lackschewitz K., Hügler M., Hannington M.D. & Gemmell J.B. (2009) - *Shallow submarine hydrothermal systems in the Aeolian volcanic arc. EOS Trans*. Am. Geophys. Union, **90**: 110-111.

Montelius C., Allen R.L., Svenson S.Å. & Weihed P. (2007) - *Facies architecture of the Palaeoproterozoic VMS-bearing Maurliden volcanic centre, Skellefte district, Sweden*. GFF, **129**: 177-196.

Morelli C., Giese P., Cassinis R., Colombi B., Guerra I., Luongo G., Scarascia S. & Schütte K.G. (1975) - *Crustal structure of southern Italy. A seismic refraction profile between Puglia-Calabria-Sicily*. Boll. Geofis. Teor. Appl, **18**: 183-210.

Morten L., Landini F., Bocchi G., Mottana A. & Brunfelt A.O. (1980) - *Fe-Mn crusts from the southern Tyrrhenian Sea*. Chem. Geol., **28**: 261-278.

Morton R.L., Walker J.S., Hudak G.J. & Franklin J.M. (1991) - *The early development of an*

Archean submarine caldera complex with emphasis on the Mattabi ash-flow tuff and its relationship to the Mattabi massive sulfide deposit. Econ. Geol., **86**: 1002-1011.

Nicolosi I., Speranza F. & Chiappini M. (2006) - *Ultrafast oceanic spreading of the Marsili basin, southern Tyrrhenian Sea: Evidence from magnetic anomaly analysis*. Geology, **34**: 717-720.

Passaro S., Milano G., D'Isanto C., Ruggieri S., Tonielli R., Bruno P.P., Sprovieri M. & Marsella E. (2010) - *DTM-based morphometry of the Palinuro seamount (eastern Tyrrhenian Sea): Geomorphological and volcanological implications*. Geomorphology, **115**: 129-140.

Peccerillo A., Frezzotti M.L., De Astis G. & Ventura G. (2006) - *Modeling the magma plumbing system of Vulcano (Aeolian islands, Italy) by integrated fluid-inclusion geobarometry, petrology, and geophysics*. Geology, **34**: 17-20.

Peters M., Strauss H., Petersen S., Kummer N.A. & Thomazo C. (2011) - *Hydrothermalism in the Tyrrhenian Sea: Inorganic and microbial sulfur cycling as revealed by geochemical and multiple sulfur isotope data*. Chem. Geol., **280**: 217-231.

Petersen S. (2014a) - *R/V Meteor cruise report M86/4: Geological setting, pore water chemistry, sediment chemistry, and metagenomics of hydrothermal systems in the Tyrrhenian Sea*. METEOR-Berichte, University of Bremen, Germany, 32 pp.

Petersen S. (2014b) - *R/V Poseidon cruise report POS442 - auvintys: High-resolution geological investigations of hydrothermal sites in the Tyrrhenian Sea using the AUV "Abyss"*. Berichte aus dem GEOMAR Helmholtz-Zentrum für Ozeanforschung Kiel, Germany, **16**, 27 pp.

Petersen S. & Monecke T. (2008) - *R/V Poseidon cruise report POS340 - TYMAS: Tyrrhenian massive sulfides*. Berichte aus dem Leibniz-Institut für Meereswissenschaften an der Christian-Albrechts-Universität zu Kiel, Germany, **21**, 73 pp.

Petersen S. & Monecke T. (2009) - *R/V Meteor cruise report M73/2 - PALINDRILL: Shallow drilling of hydrothermal sites in the Tyrrhenian Sea*. Berichte aus dem Leibniz-Institut für Meereswissenschaften an der Christian-Albrechts-Universität zu Kiel, Germany, **30**, 230 pp.

Petersen S., Monecke T., Westhues A., Hannington M.D., Gemmell J.B., Sharpe R., Peters M., Strauss H., Lackschewitz K., Augustin N., Gibson H. & Kleeberg R. (2014) - *Drilling shallow-water massive sulfides at the Palinuro volcanic complex, Aeolian island arc, Italy*. Econ. Geol., **109**: 2129-2157.

Pichler H. (1980) - *The island of Lipari*. Rend. Soc. Ital. Mineral. Petrol., **36**: 415-440.

Piercey S.J. (2015) - *A semipermeable interface model for the genesis of subseafloor replacement-type volcanogenic massive sulfide (VMS) deposits*. Econ. Geol., **110**: 1655-1660.

Puchelt H. & Laschek D. (1987) - *Massive sulphide and oxide ores in the Tyrrhenian Sea from Sonne cruise 41*. Terra Cognita, **7**, 188.

Ripepe M., Marchetti E., Ulivieri G., Harris A., Dehn J., Burton M., Caltabiano T. & Salerno G. (2005) - *Effusive to explosive transition during the 2003 eruption of Stromboli volcano*. Geology, **33**: 341-344.

Rittmann A. (1931) - *Der Ausbruch des Stromboli am 11 September 1930*. Z. Vulkanol., **14**: 47-77.

Romagnoli C. (2013) - *Characteristics and morphological evolution of the Aeolian volcanoes from the study of submarine portions*. Geol. Soc. Lond. Mem., **37**: 13-26.

Romagnoli C., Casalbore D., Bortoluzzi G., Bosman A., Chiocci F.L., D'Oriano F., Gamberi F., Ligi M. & Marani M. (2013a) - *Bathy-morpho-logical setting of the Aeolian islands*. Geol. Soc. Lond. Mem., **37**: 27-36.

Romagnoli C., Casalbore D., Bosman A., Braga R. & Chiocci F.L. (2013b) - *Submarine structure of Vulcano volcano (Aeolian islands) revealed by high-resolution bathymetry and seismo-acoustic data*. Mar. Geol., **338**: 30-45.

Romagnoli C., Kokelaar P., Rossi P.L. & Sodi A. (1993) - *The submarine extension of Sciara del Fuoco feature (Stromboli isl.): Morphologic characterization*. Acta Vulcanol., **3**: 91-98.

Rosenbaum G. & Lister G.S. (2004) - *Neogene and Quaternary rollback evolution of the Tyrrhenian Sea, the Apennines, and the Sicilian Maghrebides*. Tectonics, **23**: TC1013, doi: 10.1029/2003TC001518.

Rosi M., Pistolesi M., Bertagnini A., Landi P., Pompilio M. & Di Roberto A. (2013) - *Stromboli volcano, Aeolian islands (Italy): Present eruptive activity and hazards*. Geol. Soc. Lond. Mem., **37**: 473-490.

Rusch A., Walpersdorf E., De beer D., Gurrieri S. & Amend J.P. (2005) - *Microbial communities near the oxic/anoxic interface in the hydrothermal system of Vulcano island, Italy*. Chem. Geol., **224**: 169-182.

Ryan W.B.F., Carbotte S.M., Coplan J.O., O'Hara S., Melkonian A., Arko R., Weissel R.A., Ferrini V., Goodwillie A., Nitsche F., Bonczkowski J. & Zemsky R. (2009) - *Global multi-resolution topography synthesis*. Geochem. Geophys. Geosys., **10**, Q03014, doi: 10.1029/2008GC002332.

Safipour R., Hölz S., Halbach J., Jegen M., Petersen S. & Swidinsky A. (2017) - *A self-potential investigation of submarine massive sulfides: Palinuro seamount, Tyrrhenian Sea*. Geophysics, **82**: A51-A56.

Safipour R., Hölz S., Jegen M. & Swidinsky A. (2018) - *A first application of a marine inductive source electromagnetic configuration with remote electric dipole receivers: Palinuro seamount, Tyrrhenian Sea*. Geophys. Prospect., **66**: 1415-1432.

SAVELLI C. (1988) - *Late Oligocene to recent episodes of magmatism in and around the Tyrrhenian Sea: Implications for the processes of opening in a young inter-arc basin of intra-orogenic (Mediterranean) type*. Tectonophysics, **146**: 163-181.

SAVELLI C. (1992) - *Il rifting del vulcano Marsili (Mar Tirreno): Aspetti morfo-tettonici osservati da bordo del sottomarino "MIR 2"*. G. Geol., **54**: 215-227.

SAVELLI C. (2001) - *Two-stage progression of volcanism (8-0 Ma) in the central Mediterranean (southern Italy)*. J. Geodyn., **31**: 393-410.

SAVELLI C. (2002) - *Time-space distribution of magmatic activity in the western Mediterranean and peripheral orogens during the past 30 Ma (a stimulus to geodynamic considerations)*. J. Geodyn., **34**: 99-126.

SAVELLI C. & GASPAROTTO G. (1994) - *Calc-alkaline magmatism and rifting of the deep-water volcano of Marsili (Aeolian back-arc, Tyrrhenian Sea)*. Mar. Geol., **119**: 137-157.

SAVELLI C., MARANI M. & GAMBERI F. (1999) - *Geochemistry of metalliferous, hydrothermal deposits in the Aeolian arc (Tyrrhenian Sea)*. J. Volcanol. Geotherm. Res., **88**: 305-323.

SAVELLI C. & SCHREIDER A.A. (1991) - *The opening processes in the deep Tyrrhenian basins of Marsili and Vavilov, as deduced from magnetic and chronological evidence of their igneous crust*. Tectonophysics, **190**: 119-131.

SBORSHCHIKOV I.M. & AL´MUKHAMEDOV A.I. (1992) - *Submarine volcanoes of the Tyrrhenian Sea - Testaments to the opening of a backarc basin*. Int. Geol. Rev., **34**: 166-177.

SBORSHCHIKOV I.M., SAVELLI C. & DUKOV N. (1989) - *Side-scan sonar survey on the summit of Marsili volcano: Rifting morphology of an active axial zone in the Tyrrhenian Sea*. G. Geol., **51**: 109-116.

SCHMIDT M., LINKE P., SOMMER S., ESSER D. & CHEREDNICHENKO S. (2015) - *Natural CO_2 seeps offshore Panarea: A test site for subsea CO_2 leak detection technology*. Mar. Technol. Soc. J., **49**: 19-30.

SEDWICK P. & STÜBEN D. (1996) - *Chemistry of shallow submarine warm springs in an arc-volcanic setting: Vulcano island, Aeolian archipelago, Italy*. Mar. Chem., **53**: 147-161.

SELLI R., LUCCHINI F., ROSSI P.L., SAVELLI C. & DEL MONTE M. (1977) - *Dati geologici, petrochimici e radiometrici sui vulcani centro-tirrenici*. G. Geol., **42**: 221-246.

SILLITOE R.H. & HEDENQUIST J.W. (2003) - *Linkages between volcanotectonic settings, ore-fluid compositions, and epithermal precious metal deposits*. SEG Spec. Pub., **10**: 315-343.

SMYTH W.H. (1824) - *Memoir descriptive of the resources, inhabitants, and hydrography, of Sicily and its islands, interspersed with antiquarian and other notices*. J. Murray, London, 291 pp.

SOLÌGO M., DE ASTIS G., DELITALA M.C., LA VOLPE L., TADDEUCCI A. & TUCCIMEI P. (2000) - *Uranium-series disequilibria in the products from Vulcano island (Sicily, Italy): Isotopic chronology and magmatological implications*. Acta Vulcan., **12**: 49-59.

STOFFERS P., WORTHINGTON T.J., SCHWARZ-SCHAMPERA U., HANNINGTON M.D., MASSOTH G.J., HEKINIAN R., SCHMIDT M., LUNDSTEN L.J., EVANS L.J., VAIOMO'UNGA R. & KERBY T. (2006) - *Submarine volcanoes and high-temperature hydrothermal venting on the Tonga arc, southwest Pacific*. Geology, **34**: 453-456.

STÜBEN D., BLOOMER S.H., TAÏBI N.E., NEUMANN T., BENDEL V., PÜSCHEL U., BARONE A., LANGE A., SHIYING W., CUIZHONG L. & DEYU Z. (1992) - *First results of study of sulphur-rich hydrothermal activity from an island-arc environment: Esmeralda Bank in the Mariana arc*. Mar. Geol., **103**: 521-528.

SVENSSON E., SKOOG A. & AMEND J.P. (2004) - *Concentration and distribution of dissolved amino acids in a shallow hydrothermal system, Vulcano island (Italy)*. Org. Geochem., **35**: 1001-1014.

SZITKAR F., PETERSEN S., CARATORI TONTINI F. & COCCHI L. (2015) - *High-resolution magnetics reveal the deep structure of a volcanic-arc-related basalt-hosted hydrothermal site (Palinuro, Tyrrhenian Sea)*. Geochem. Geophys. Geosys. **16**: 1950-1961.

TAMBURELLI C., BABBUCCI D. & MANTOVANI E. (2000) - *Geodynamic implications of "subduction related" magmatism: Insights from the Tyrrhenian-Apennines region*. J. Volcanol. Geotherm. Res., **104**: 33-43.

TARQUINI S. & NANNIPIERI L. (2017) - *The 10 m-resolution TINITALY DEM as a trans-disciplinary basis for the analysis of the Italian territory: Current trends and new perspectives*. Geomorphology, **281**: 108-115.

TASSI F., CAPACCIONI B., CARAMANNA G., CINTI D., MONTEGROSSI G., PIZZINO L., QUATTROCCHI F. & VASELLI O. (2009) - *Low-ph waters discharging from submarine vents at Panarea island (Aeolian islands, southern Italy) after the 2002 gas blast: Origin of hydrothermal fluids and implications for volcanic surveillance*. Appl. Geochem., **24**: 246-254.

TASSI F., CAPACCIONI B. & VASELLI O. (2014) - *Compositional spatial zonation and 2005-2013 temporal evolution of the hydrothermal-magmatic fluids from the submarine fumarolic field at Panarea island (Aeolian archipelago, southern Italy)*. J. Volcanol. Geotherm. Res., **277**: 41-50.

THIEL V., HÜGLER M., BLÜMEL M., BAUMANN H.I., GÄRTNER A., SCHMALJOHANN R., STRAUSS H., GARBE-SCHÖNBERG D., PETERSEN S., COWART D.A., FISHER C.R. & IMHOFF J.F. (2012) - *Widespread occurrence of two carbon fixation pathways in tubeworm endosymbionts: Lessons from hydrothermal vent associated tubeworms from the Mediterranean Sea*. Front. Microbiol., **3**, 423, doi: 10.3389/fmicb.2012.00423.

TOR J.M., AMEND J.P. & LOVLEY D.R. (2003) - *Me-*

tabolism of organic compounds in anaerobic, hydrothermal sulphate-reducing marine sediments. Environ. Microbiol., **5**: 583-591.

TRUA T., SERRI G., MARANI M., RENZULLI A. & GAMBERI F. (2002) - *Volcanological and petrological evolution of Marsili seamount (southern Tyrrhenian Sea)*. J. Volcanol. Geotherm. Res., **114**: 441-464.

TUFAR W. (1991) - *Paragenesis of complex massive sulfide ores from the Tyrrhenian Sea: Mitt*. Österr. Geol. Ges., **84**: 265-300.

UCHUPI E. & BALLARD R.D. (1989) - *Evidence of hydrothermal activity on Marsili seamount, Tyrrhenian basin*. Deep-Sea Res., **36**: 1443-1448.

UCHUPI E., GALLO D.G. & BALLARD R.D. (1988) - *Hydrothermal activity on the crest of Marsili seamount, Tyrrhenian basin imaged with a video system*. EOS Trans. Am. Geophys. Union, **69**, 1270.

VALETTE J.N. (1973) - *Distribution of certain trace elements in marine sediments surrounding Vulcano island (Italy)*. In: AMSTUTZ G.C. & BERNARD A.J. (Eds), Ores in Sediments. Springer, Berlin, 321-337.

VALSAMI-JONES E., BALTATZIS E., BAILEY E.H., BOYCE A.J., ALEXANDER J.L., MAGGANAS A., ANDERSON L., WALDRON S. & RAGNARSDOTTIR K.V. (2005) - *The geochemistry of fluids from an active shallow submarine hydrothermal system: Milos island, Hellenic volcanic arc*. J. Volcanol. Geotherm. Res., **148**: 130-151.

VENTURA G. (1994) - *Tectonics, structural evolution and caldera formation on Vulcano island (Aeolian archipelago, southern Tyrrhenian Sea)*. J. Volcanol. Geotherm. Res., **60**: 207-224.

VENTURA G., VILARDO G., MILANO G. & PINO N.A. (1999) - *Relationships among crustal structure, volcanism and strike-slip tectonics in the Lipari-Vulcano volcanic complex (Aeolian islands, southern Tyrrhenian Sea, Italy)*. Phys. Earth Planet. Inter., **116**: 31-52.

VOLTATTORNI N., SCIARRA A., CARAMANNA G., CINTI D., PIZZINO L. & QUATTROCCHI F. (2009) - *Gas geochemistry of natural analogues for the studies of geological CO_2 sequestration*. Appl. Geochem., **24**: 1339-1346.

WANG C.Y., HWANG W.T. & SHI Y. (1989) - *Thermal evolution of a rift basin: The Tyrrhenian Sea*. J. Geophys. Res., **94**: 3991-4006.

WAUSCHKUHN A. & GRÖPPER H. (1975) - *Rezente Sulfidbildung auf und bei Vulcano, Äolische Inseln, Italien*. N. Jb. Miner. Abh., **126**: 87-111.

WHITE N.C. & HEDENQUIST J.W. (1995) - *Epithermal gold deposits: Styles, characteristics and exploration*. SEG Newsl., **23**: 1, 9-13.

WRIGHT I.C., DE RONDE C.E.J., FAURE K. & GAMBLE J.A. (1998) - *Discovery of hydrothermal sulfide mineralization from southern Kermadec arc volcanoes (SW Pacific)*. Earth Planet. Sci. Lett., **164**: 335-343.

YANG T.F., LAN T.F., LEE H.F., FU C.C., CHUANG P.C., LO C.H., CHEN C.H., CHEN C.T.A. & LEE C.S. (2005) - *Gas compositions and helium isotopic ratios of fluid samples around Kueishantao, NE offshore Taiwan and its tectonic implications*. Geochem. J., **39**: 469-480.